Dynamic quantum circuit compilation

Kun Fang[1], Munan Zhang[1], Ruqi Shi[1], and Yinan Li[2]

[1]Institute for Quantum Computing, Baidu Research, Beijing 100193, China
[2]School of Mathematics and Statistics and Hubei Key Laboratory of Computational Science, Wuhan University, Wuhan 430072, China

Quantum computing has shown tremendous promise in addressing complex computational problems, yet its practical realization is hindered by the limited availability of qubits for computation. Recent advancements in quantum hardware have introduced mid-circuit measurements and resets, enabling the reuse of measured qubits and significantly reducing the qubit requirements for executing quantum algorithms. In this work, we present a systematic study of dynamic quantum circuit compilation, a process that transforms static quantum circuits into their dynamic equivalents with a reduced qubit count through qubit-reuse. We establish the first general framework for optimizing the dynamic circuit compilation via graph manipulation. In particular, we completely characterize the optimal quantum circuit compilation using binary integer programming, provide efficient algorithms for determining whether a given quantum circuit can be reduced to a smaller circuit and present heuristic algorithms for devising dynamic compilation schemes in general. Furthermore, we conduct a thorough analysis of quantum circuits with practical relevance, offering optimal compilations for well-known quantum algorithms in quantum computation, ansatz circuits utilized in quantum machine learning, and measurement-based quantum computation crucial for quantum networking. We also perform a comparative analysis against state-of-the-art approaches, demonstrating the superior performance of our methods in both structured and random quantum circuits. Our framework lays a rigorous foundation for comprehending dynamic quantum circuit compilation via qubit-reuse, bridging the gap between theoretical quantum algorithms and their physical implementation on quantum computers with limited resources.

Contents

Kun Fang: fangkun02@baidu.com

1 Introduction

Quantum computing has emerged as a promising avenue for solving intractable problems that are beyond the reach of classical computing, such as integer factoring [Sho94], large database search [Gro96], chemistry simulation [LWG+10] and machine learning [BWP+17]. Nevertheless, existing quantum computers are limited by the number of qubits available for computation. To conclusively demonstrate the computational advantage of these devices compared to their classical counterparts in a variety of practical applications, we need to make efficient use of qubits when designing quantum algorithms.

A plethora of quantum algorithms have been traditionally formulated as *static quantum circuits*, where the computation is performed on an initially prepared quantum state, and all measurements are applied at the end of the circuit to extract the computational results. However, the recent advancements in quantum hardware have paved the way for a more flexible approach, allowing for measurements and qubit resets to be executed in the midst of a quantum circuit. Moreover, these dynamic circuits permit the real-time evolution of the quantum circuit based on prior measurement outcomes [CTI+21, PDF+21, AI23]. This new paradigm of quantum computation, characterized by the ability to dynamically adjust the circuit, is referred to as a *dynamic quantum circuit*, and plays a crucial role in the study of quantum error correction [FMMC12], quantum communication [BBC+93], and also measurement-based quantum computation [RB01].

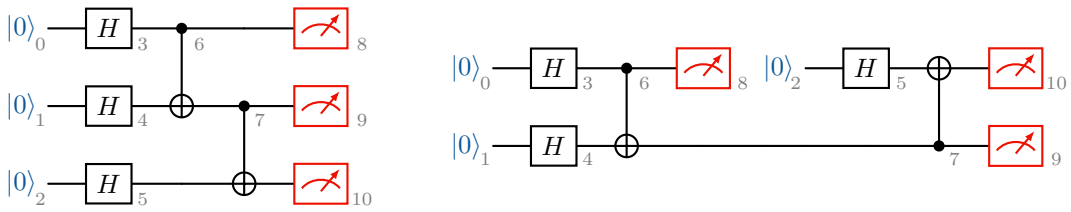

(a) A static quantum circuit with 3 qubits.

(b) A dynamic quantum circuit with 2 qubits.

Figure 1: An example of dynamic quantum circuit compilation from (a) to (b).

This work investigates dynamic quantum circuit compilation, which rewires static quantum circuits into equivalent dynamic circuits using fewer qubits through qubit-reuse strategies. An explicit example is illustrated in Figure 1, where a 3-qubit static quantum circuit is compiled into a 2-qubit dynamic circuit by recycling the first qubit following its measurement instruction and subsequently reusing it for operations on the third qubit of the original static circuit. The idea of compiling a quantum circuit via qubit-reuse was first introduced in [PWD16], which employed the notion of wire recycling applied to predefined ancilla qubits. Subsequently, the work in [DCKFF22] studied quantum circuit compilation using the causal structure of the circuits and formulated the optimal qubit reuse as a constraint programming and satisfiability problem for small circuits. Additionally, it introduced a greedy algorithm tailored for large quantum circuits. In [HJC+23], the authors designed a compiler-assisted tool that exploits the trade-off between qubit reuse, fidelity, gate count, and circuit duration. They also conducted experiments on quantum hardware, demonstrating that dynamic circuit compilation indeed achieved an improvement in qubit usage and circuit fidelity for select applications. In [BPK23], the authors introduced an SAT-based model for qubit reuse optimization on near-term quantum devices. However, their approach encountered computational challenges and scalability issues as the number of qubits increased.

In general, dynamic quantum circuit compilation via qubit-reuse offers substantial advantages and addresses several critical facets of fault-tolerant quantum computation. Firstly, it efficiently reduces the number of qubits required for executing certain quantum algorithms, which is particularly valuable for the practical implementation of large-scale quantum circuits on near-term quantum computers and enhances the feasibility of their classical simulation. Besides, by compacting the quantum circuit topology, qubit-reuse effectively simplifies the complexity of the circuits. This simplification holds the potential to minimize the need for inserting swap gates when mapping

logical circuits to specific quantum hardware devices, ultimately resulting in error reduction and fidelity improvements [HJC+23, BPK23]. Furthermore, determining the minimum number of qubits needed for executing specific quantum algorithms provides profound insights into the algorithms' complexity, helping to design efficient algorithms with quantum advantages.

It is worth noting that circuit optimization manifests in various forms, typically entailing modifications to the gate structure of a quantum circuit with the goal of enhancing result fidelity. These modifications encompass strategies such as reducing gate count by simplifying Clifford subcircuits [AG04, BSHM21], eliminating redundant gates [con23, XMP+23, XLP+22], and applying the Cartan decomposition to two-qubit gates [KG00]. Furthermore, circuit optimization may encompass the mapping of circuits to a specific quantum device architecture, aiming to minimize potential transport or swap gate costs [con23, ZPW18]. In contrast, dynamic quantum circuit compilation is centered around the reordering of instructions and the reassignment of logical qubits, while preserving both the number and type of circuit instructions. This approach serves as a complementary strategy to other circuit optimization techniques and can integrate with the existing ones. For instance, it can be applied after the removal of redundant gates or before the mapping of the circuit to a specific quantum hardware architecture.

In this work, we conduct a comprehensive investigation into dynamic quantum circuit compilation, a process that transforms a static quantum circuit into an equivalent dynamic circuit with a reduced qubit count through qubit-reuse. Notably, we introduce the first general framework for optimizing dynamic circuit compilation through graph manipulation. This approach enables us to efficiently assess the reducibility of a static quantum circuit, derive optimal compilations for various practical quantum algorithms, and design heuristic algorithms that outperform existing methods. The structure of this work is as follows: Section 2 introduces the notations and fundamental concepts employed throughout our study. Section 3 briefly outlines the fundamentals of quantum circuits and their different representations. In Section 4, we formulate the foundation for dynamic quantum circuit compilation through graph manipulation, establishing a crucial framework for subsequent discussions. Section 5 delves into various efficient approaches for determining the reducibility of a static quantum circuit. Section 6 transforms the graph optimization problem into a binary integer programming problem, offering a rigorous mathematical framework for optimal quantum circuit compilation. Due to the complexity of finding optimal solutions, we propose several heuristic algorithms in Section 7. Section 8 features a thorough analysis of quantum circuits with practical relevance, providing optimal compilations for well-known quantum algorithms in quantum computation, ansatz circuits applied in quantum machine learning, and measurement-based quantum computation crucial for quantum networking. We also present a comparative analysis against state-of-the-art approaches, highlighting the superior performance of our methods in both structured and random quantum circuits. Finally, Section 9 concludes our study and explores related open problems.

It is worth mentioning that the main algorithms presented in this work have been implemented in QNET, a quantum network toolkit developed by the Institute for Quantum Computing at Baidu. All the code referenced in this paper can be accessed online on GitHub [1].

2 Preliminaries

2.1 Notation

In the table below, we briefly summarize the notation which we use throughout this work.

[1] https://github.com/baidu/QCompute/tree/master/Extensions/QuantumNetwork

Symbol	Definition
I_n	identity matrix of size $n \times n$
J_n	all-one matrix of size $n \times n$
O_n	zero matrix of size $n \times n$
$E_{i,j}^k$	$k \times k$ matrix whose (i,j)-th entry is one and zero otherwise
n	width of quantum circuit
m	number of quantum instructions
q_i	qubit with index i
$A(G)$	adjacency matrix of graph G
$B(G)$	biadjacency matrix of bipartite graph G
r, t	roots and terminals in the graph representation of a quantum circuit
(u, v)	directed edge from u to v
$\delta^-(v)$	indegree of vertex v
$\delta^+(v)$	outdegree of vertex v
log	logarithm of base 2
$list[i]$	the i-th element of a list

Table 1: Overview of notational conventions.

Note that we adopt the convention that all qubit registers in quantum circuits, along with the row and column indices of matrices, and the indices of lists in algorithms, all start from zero.

2.2 Graph theory

A graph is an ordered pair $G = (V, E)$ comprising a set of vertices V and a set of edges E. A graph is directed if its edges are ordered pairs of vertices. For any edge (u, v) in a directed graph, u is called the tail and v is called the head of the edge. For a vertex v, the number of head ends adjacent to a vertex is called the indegree of the vertex which is denoted as $\delta^-(v)$ and the number of tail ends adjacent to a vertex is its outdegree, which is denoted as $\delta^+(v)$. A vertex with zero indegree is called a root and a vertex with zero outdegree is called a terminal. A vertex v is *reachable* from another vertex u if there exists a direct path from u to v in the graph. A *directed acyclic graph* (DAG) is a directed graph with no directed cycles, which has been widely used in formulating the classical and quantum circuit model. A *topological ordering* of a DAG is an ordering of its vertices into a sequence, such that for every edge the tail vertex of the edge occurs earlier in the sequence than the head vertex of the edge. In general, this ordering can be efficiently obtained from its DAG but the result ordering is not unique. A *bipartite graph* is a graph whose vertices can be divided into two disjoint and independent sets U and V such that every edge connects a vertex in set U to a vertex in set V. We write $G = (U, V, E)$ to denote a bipartite graph whose partition has the parts U and V, with E denoting the edges of the graph. A bipartite graph is complete if every vertex in U is connected to every vertex in V.

2.3 Boolean matrix

A Boolean matrix is a matrix whose entries are either 0 or 1. Let A and B be two Boolean matrices of size $k \times k$. Then their Boolean product is defined as

$$(A \odot B)_{ij} := \bigvee_{l=0}^{k-1} (A_{il} \wedge B_{lj}), \tag{1}$$

where $\vee$ is the logical OR and $\wedge$ is the logical AND. Let $G = (V, E)$ be a directed graph where $V = \{v_0, \cdots, v_{k-1}\}$. Its *adjacency matrix* is a Boolean matrix, denoted as $A(G)$, of size $k \times k$ whose elements indicate whether pairs of vertices are adjacent or not in the graph. That is, the (i, j)-th entry of the adjacency matrix is one if the directed edge $(v_i, v_j) \in E$ and zero otherwise.

If a bipartite graph $G = (U, V, E)$ with $U = \{u_0, \cdots, u_{k-1}\}$, $V = \{v_0, \cdots, v_{k-1}\}$ and all edges pointing from part U to part V, then its adjacency matrix can be written in the form:

$$A(G) = \begin{pmatrix} O_k & X \\ O_k & O_k \end{pmatrix} \tag{2}$$

where X is an $k \times k$ Boolean matrix in which $X_{ij} = 1$ if $(u_i, v_j) \in E$. We call this submatrix the *biadjacency matrix* of the bipartite graph and denote it as $B(G)$. Note that the biadjacency matrix of a complete bipartite graph is an all-one matrix.

A matrix A of size $k \times k$ is *nilpotent* if there exists an integer l with $1 \leq l \leq k$ such that $A^l = O_k$. The following result gives a characterization of DAG by its adjacency matrix (see [LQW+22] or [Deo16, Theorem 9-17]).

Lemma 1 *A directed graph is acyclic if and only if its adjacency matrix is nilpotent.*

3 Quantum circuit and its representations

A quantum circuit is a mathematical and visual model used in quantum computing to represent and perform quantum computations. It is analogous to classical digital circuits used in classical computing. A quantum circuit consists of a series of quantum gates, each of which operates on one or more qubits. In this work, we focus on single-qubit and two-qubit gates without loss of generality and most of the results apply to multi-qubit gates with slight modification. A quantum circuit is *static* if it does not contain mid-circuit reset operations and all measurements, are performed at the end of the circuit (e.g., Figure 1a). A quantum circuit is *dynamic* if it contains mid-circuit measurements and reset operations (e.g., Figure 1b). A quantum circuit is *reducible* if it can be written as an equivalent quantum circuit with fewer qubits. Otherwise, it is called *irreducible*. A quantum circuit and its reduced circuit are considered equivalent if their measurement outcomes yield identical distributions. Consequently, no classical post-processing of the circuits' output can differentiate between them [DCKFF22].

3.1 Quantum circuit instructions

Quantum circuits are conventionally depicted through circuit diagrams. Nevertheless, when considering circuit compilation, a more precise and streamlined approach involves employing quantum circuit instructions. This allows a quantum circuit to be presented as a list of instructions, structured according to the chronological order of their execution. Each entry within the instruction list corresponds to a distinct quantum operation within the circuit and is denoted by a quartet [ID, TYPE, QUBIT, PAR]. This quartet serves to uniquely identify the operation, specify its operation type, indicate the qubit(s) it acts upon, and provide any relevant parameters (set to 'NONE' in cases where no parameters are applicable) [FZL+23]. For example, the instruction [5, RY, 1, π] signifies the application of an R_y rotation gate to qubit q_1, with the rotation angle set to π, and the corresponding instruction ID is 5. Similarly, the instruction [4, CX, [0, 2], NONE] represents the implementation of a controlled-NOT gate, with q_0 as the control qubit and q_2 as the target qubit, with an instruction ID of 4. Likewise, the instruction [7, MEASURE, 2, NONE] denotes the measurement of qubit q_2 in the computational basis, with an instruction ID of 7. Finally, the instruction [2, RESET, 3, NONE] indicates the reset of qubit q_3 to the ground state, typically represented as the zero state, and carries an instruction ID of 2. An example of quantum circuit instructions is given in Figure 2.

3.2 Graph representation of quantum circuit

Considering that a quantum circuit essentially constitutes a time-ordered sequence of quantum instructions, it is natural to employ a directed graph to represent the causal relationships among them. In this context, a quantum circuit finds its representation through a directed graph, effectively preserving the execution constraints of all quantum instructions. To be more specific, each quantum instruction corresponds to a vertex within the graph. A directed edge starting

Quantum Circuit Instructions

ID	TYPE	QUBIT	PAR
0	RESET	0	NONE
1	RESET	1	NONE
2	RESET	2	NONE
3	H	0	NONE
4	H	1	NONE
5	H	2	NONE
6	CX	[0, 1]	NONE
7	CX	[1, 2]	NONE
8	MEASURE	0	NONE
9	MEASURE	1	NONE
10	MEASURE	2	NONE

(a) Instructions for quantum circuit in Figure 1a.

Quantum Circuit Instructions

ID	TYPE	QUBIT	PAR
0	RESET	0	NONE
1	RESET	1	NONE
3	H	0	NONE
4	H	1	NONE
6	CX	[0, 1]	NONE
8	MEASURE	0	NONE
2	RESET	0	NONE
5	H	0	NONE
7	CX	[1, 0]	NONE
10	MEASURE	0	NONE
9	MEASURE	1	NONE

(b) Instructions for quantum circuit in Figure 1b.

Figure 2: An example of quantum circuit instructions. For clarity, RESET instructions are highlighted in blue, and MEASURE instructions are indicated in red.

from vertex u and terminating at vertex v signifies that the quantum instruction associated with vertex u must be executed before the quantum instruction associated with vertex v. Crucially, this directed graph is inherently acyclic, as the presence of any cycle would imply a dependency of past instructions on future ones, contravening the causal relationship inherent in the quantum circuit. Given this characteristic, we refer to this directed graph as the *DAG representation* of the quantum circuit (see e.g. Figure 3b).

In this work, we will employ the DAG representation to investigate the dynamic quantum circuit compilation problem. To facilitate our analysis, all vertices within the DAG representation can be categorized into three distinct groups:

1. Root vertices: vertices with zero indegree, which correspond to the first layer of quantum operations on each qubit (typically reset operations);
2. Terminal vertices: vertices with zero outdegree, which correspond to the last layer of quantum operations on each qubit (typically quantum measurements);
3. Internal vertices: vertices with nonzero indegree and outdegree, which correspond to the intermediate quantum operations (typically quantum gates).

Remark 1 We assume that all static quantum circuits in this work start from reset operations and end with measurements. This implies that the circuit width is equal to the number of root vertices within the DAG representation.

In Algorithm 1 below, we present an efficient procedure for transforming a quantum circuit from its circuit instructions into the corresponding DAG representation. The time complexity of this algorithm is $O(m)$, with m denoting the total number of circuit instructions.

Concerning our compilation problem, all essential information resides within the reachability from roots to terminals within the DAG representation, while the internal vertices facilitate and transmit this reachability. Consequently, we can further streamline the DAG representation, concentrating our focus on the *simplified DAG representation* of the circuit. This simplified representation takes the form of a bipartite graph (R, T, E), with R and T representing the sets of roots and terminals from the DAG representation. An edge (r, t) in E connects a root $r \in R$ to a terminal $t \in T$ if a directed path exists from r to t within the DAG representation. To illustrate this concept, Figure 3 showcases an example of a quantum circuit alongside its corresponding DAG and simplified DAG representations.

Algorithm 1: Converting static quantum circuit to DAG

Input:

StaticCircuit a static quantum circuit instructions

Output:

Digraph a DAG representation of the static quantum circuit

```
Let n be the width of quantum circuit;
Initialize an empty directed graph Digraph;
Initialize a list CausalLists of length n, with each element initialized as an empty list;
foreach Instruction in StaticCircuit do
    Add a vertex Vertex labeled as ID of Instruction to Digraph;
    foreach q in QUBIT value of instruction do
        Find the last entry of CausalLists[q] and record it as PreVertex;
        if PreVertex exits then
            Add a directed edge to Digraph, pointing from PreVertex to Vertex;
        end
        Append ID of Instruction to the end of list CausalLists[q];
    end
end
return Digraph
```

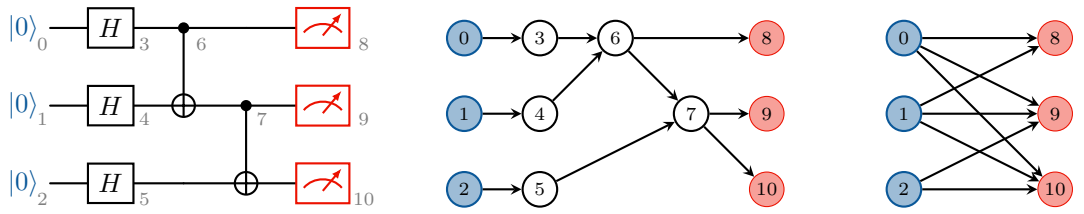

(a) Quantum circuit diagram. (b) Directed acyclic graph (DAG). (c) Simplified DAG.

Figure 3: An example of a quantum circuit and its DAG and simplified DAG representations. Root vertices are marked in blue, terminal vertices in red and internal vertices in white.

3.3 Quantum circuit composition and subcircuit

Quantum circuit composition stands as a fundamental technique for integrating modular components into complex quantum algorithms. An illustrative instance arises in the domain of quantum machine learning, exemplified by the Variational Quantum Eigensolver (VQE) [PMS+14] and Quantum Approximate Optimization Algorithm (QAOA) [FGG14] where specific quantum circuit patterns are joined sequentially. More specifically, given two quantum circuits of the same size, we define their *circuit composition* as the sequential integration of quantum gate operations from a second circuit onto those of the first, while preserving the initialization in the first circuit and the measurement in the second. An illustration of quantum circuit composition and the sequence of circuit instructions is presented in Figure 4. Conversely, we can also consider *subcircuits* which are obtained by removing part of circuit instructions from the original circuit. This approach offers an alternative perspective for gaining insight into the essential structure of the circuit.

4 Quantum circuit compilation via graph manipulation

In this section, we present the mathematical formulation of the quantum circuit compilation problem using its graph representation, which serves as a pivotal foundation for subsequent in-depth investigations. Drawing inspiration from the example illustrated in Figure 1, dynamic quantum

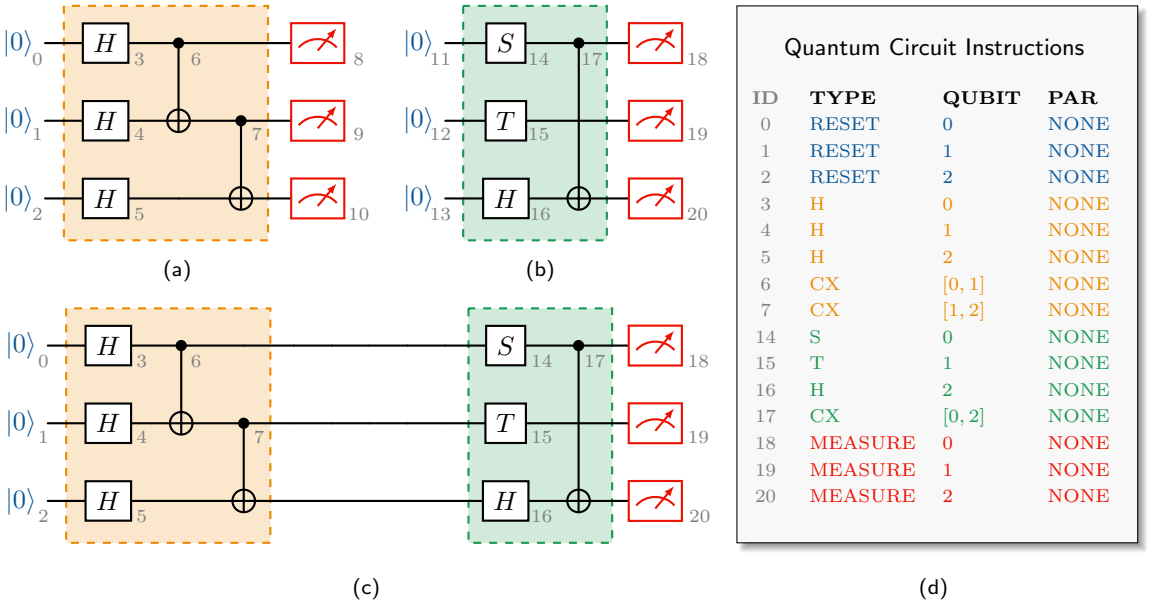

ID	TYPE	QUBIT	PAR
0	RESET	0	NONE
1	RESET	1	NONE
2	RESET	2	NONE
3	H	0	NONE
4	H	1	NONE
5	H	2	NONE
6	CX	[0, 1]	NONE
7	CX	[1, 2]	NONE
14	S	0	NONE
15	T	1	NONE
16	H	2	NONE
17	CX	[0, 2]	NONE
18	MEASURE	0	NONE
19	MEASURE	1	NONE
20	MEASURE	2	NONE

Figure 4: An illustration of quantum circuit composition. (a) the diagram of the first quantum circuit; (b) the diagram of the second quantum circuit; (c) the diagram of the composite quantum circuit; (d) the instructions of the composite quantum circuit.

circuit compilation via qubit-reuse involves resetting a qubit after measurement, thereby deferring certain reset operations until after the measurement process. In the DAG representation, this corresponds to the addition of a directed edge from a terminal to a root, signifying that the corresponding reset operation occurs subsequent to the execution of the measurement.

For clarity, Figure 5b provides a DAG representation of the quantum circuit depicted in Figure 1a or Figure 5a. The qubit-reuse in Figure 1b is depicted by the addition of a new edge (represented as a dashed green line) from terminal 8 to root 2. With the inclusion of this new edge, the resulting DAG exactly mirrors the DAG representation of the dynamic quantum circuit portrayed in Figure 1b. This new edge can also be similarly integrated into the simplified DAG representation as demonstrated in Figure 5c.

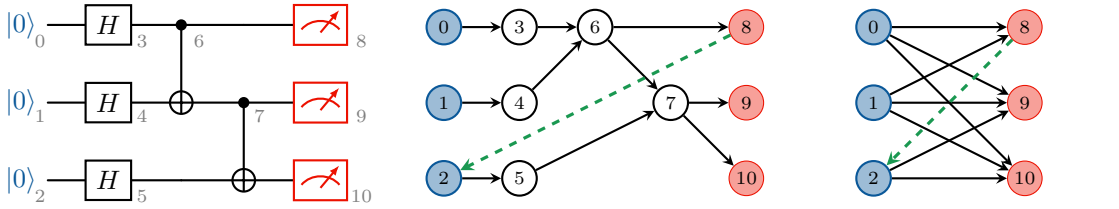

(a) quantum circuit diagram (b) DAG with new edge (c) simplified DAG with new edge

Figure 5: An illustration of quantum circuit compilation via graph manipulation. Root vertices are marked in blue, and terminal vertices in red. The newly added edge is marked in green, pointing from a terminal to a root.

The above idea of dynamic quantum circuit compilation is formally formulated as follows.

Theorem 2 *Let $G = (R, T, E)$ be the simplified DAG of a static quantum circuit. Then compiling the quantum circuit via qubit-reuse is equivalent to adding edges to G (Let E' be the set of added edges) such that*

- $\forall\ (t, r) \in E'$, *it has* $t \in T$ *and* $r \in R$;

- $\forall\ (t, r) \in E'$, *it has* $\delta^+(t) = 1$ *and* $\delta^-(r) = 1$;
- $G' = (R \cup T, E \cup E')$ *is an acyclic graph.*

The new graph G' *will be called the modified DAG in the subsequent discussion.*

Proof Dynamic quantum circuit compilation through qubit-reuse seeks to delay certain reset operations until after the measurements, which is illustrated by the addition of a directed edge from a terminal to a root in the DAG representation. However, when incorporating new edges, it is imperative to adhere to the following constraints.

1. Resetting a qubit is possible only when all operations on it have been carried out. So the added edge should start from terminals. Moreover, the circuit width is determined by the number of roots in the DAG representation. To reduce the circuit width, the added edges should end at roots. Overall, the directed edges should be added from terminals to roots. This corresponds to the first condition in the asserted result.

2. A reused qubit can only accommodate one reset operation. So the added edges should have no common tails. Moreover, since the circuit width is determined by the number of roots in the DAG representation, the added edges having common heads will not help. So we can restrict our attention to the case that the added edges share no common heads. This corresponds to the second condition in the asserted result.

3. Since directed edges represent the execution order of operations, the presence of any cycle in the graph indicates a dependency of past operations on future ones, which violates the causal relation of the quantum circuit. Therefore, the addition of these directed edges must not introduce any cycles, indicating the compiled circuit is still well-defined. This corresponds to the third condition in the asserted result.

Conversely, for any graph manipulation that complies with the specified conditions, we can demonstrate that it corresponds to a dynamic circuit compilation approach as explicitly detailed in Algorithm 2. Given that the DAG representation preserves the execution order of quantum operations within the corresponding quantum circuit, employing topological sorting on the modified DAG enables us to establish a viable execution sequence. This sequence is then utilized to rearrange the circuit instruction list. Since our actions solely involve rewiring the original quantum circuit, the resulting compiled circuit maintains its equivalence to the static circuit. Ultimately, it's worth noting that all the conditions mentioned remain independent of whether we are working with a DAG or a simplified DAG representation. ■

The time complexity of Algorithm 2 is analyzed as follows. Assume that the input static circuit has n qubits and m operations. Initially, the modified DAG is topologically sorted using the Depth-First Search (DFS) algorithm. Denoting the number of vertices and edges in the modified DAG as $|V|$ and $|E|$, it is clear that $|V| = m$. As each operation introduces at most two edges to the graph, $|E|$ scales linearly with m, resulting in $|E| = O(m)$. Consequently, the time complexity of topological sorting with DFS is $O(|V| + |E|) = O(m)$ [BJG08]. Following this, a traversal of the topological order with m vertices is performed to reorder the static circuit instructions. Note that the ID of an instruction and the label of the corresponding vertex are the same. Therefore for each vertex label i, the corresponding instruction is accessed through $\mathit{StaticCircuit}[i]$ and appended to *DynamicCircuit*, which allows the rearrangement to be completed in $O(m)$ time. Subsequently for each added edges, we need to traverse the *DynamicCircuit* list and update the qubit indices. For a static circuit with n qubits, at most $n - 1$ edges can be added to the DAG, therefore the updating step exhibits a time complexity of $O(mn)$. Consequently, the overall time complexity of Algorithm 2 is computed as $O(m) + O(m) + O(mn) = O(mn)$.

As an example, using Algorithm 2 and the modified DAG in Figure 5b, the static quantum circuit instructions in Figure 2a would be compiled to the instructions in Figure 2b.

Algorithm 2: Converting modified DAG to dynamic quantum circuit

Input:

StaticCircuit	the instruction list of a static quantum circuit
ModifiedGraph	a modified DAG
AddedEdges	a list of added edges

Output:

DynamicCircuit	the compiled dynamic quantum circuit instructions

Initialize empty lists *TopologicalOrder* and *DynamicCircuit*;
Apply topological sorting to *ModifiedGraph*, record the result in *TopologicalOrder*;
Rearrange the order of instructions in *StaticCircuit* according to the order of vertices in *TopologicalOrder*, record the result in *DynamicCircuit*;
foreach *Edge* **in** *AddedEdges* **do**
    Let v_i and v_j be the head and tail vertices of *Edge*, respectively;
    Identify the circuit instructions corresponding to v_i and v_j, record the QUBIT values of these two instructions as q_i and q_j, respectively;
    foreach *Instruction* **in** *DynamicCircuit* **do**
        foreach *Qubit* **in** *QUBIT value of Instruction* **do**
            if *Qubit is equal to* q_i **then** update *Qubit* to q_j;
        end
    end
end
return *DynamicCircuit*

Remark 2 Theorem 2 shows that dynamic quantum circuit compilation only depends on the simplified DAG representation, which is independent of the single-qubit gates in the static quantum circuit to compile. So we will omit all single-qubit gates in the subsequent discussion.

5 Determine the reducibility of quantum circuit

The preceding section has established the mathematical framework essential for understanding the complexities of dynamic quantum circuit compilation through graph manipulation. Theorem 2 indicates that this compilation process involves the deliberate addition of edges to the simplified DAG, guided by three distinct conditions. Before finding a compilation strategy for a given quantum circuit, it is crucial to determine whether this circuit is reducible at all.

In this section, we present three distinct approaches for assessing the reducibility of a static quantum circuit. The first approach is rooted in the DAG representation of the quantum circuit, while the second approach involves a direct and comprehensive analysis of the circuit's structure, guided by a set of critical observations. Departing from these geometric perspectives, the third approach utilizes Boolean matrices to discern reducibility.

5.1 Approach 1: determine the reducibility from graph

It is clear from Theorem 2 that a quantum circuit is reducible if and only if we can add at least one more edge to its DAG while adhering to the three specified conditions. This idea can be elaborated upon as follows:

Proposition 3 *A static quantum circuit is irreducible if and only if its simplified DAG is a complete bipartite graph.*

Proof If the simplified DAG $G = (R, T, E)$ is a complete bipartite graph, then any terminal is reachable from any root. Within such a graph, the inclusion of any additional edge from a terminal to a root necessarily introduces a directed cycle, thus violating the conditions. Therefore, the circuit width can not be reduced through qubit reuse. Conversely, if the simplified DAG is not complete, it indicates the absence of connections between certain roots and terminals. More specifically, there exists at least one terminal t that is not reachable from a root r. In this case, the directed edge (t, r) can be added to the graph, which does not introduce any cycles. Thereby, the corresponding circuit can be reduced to a circuit with a smaller width. ■

This result shows that the reducibility of a static quantum circuit can be completely determined by its simplified DAG. In particular, we only need to check if the biadjacency matrix of the simplified DAG is an all-one matrix. For this, we can exploit DFS algorithm to identify all paths from roots to terminals for a given DAG. The detailed algorithm of this approach along with its time complexity analysis is given in Algorithm 3 and Proposition 4.

Algorithm 3: Determining reducibility from graph

Input:

StaticCircuit	the instruction list of a static quantum circuit

Output:

True or *False*	whether the static quantum circuit is reducible

```
Run Algorithm 1 to obtain the DAG of StaticCircuit and record it as Digraph;
Let Roots and Terminals be the set of roots and terminals in Digraph, respectively;
Let n be the length of Roots and Terminals;
Initialize a n × n zero matrix B;
for i = 0 to n − 1 do
    for j = 0 to n − 1 do
        Apply DFS algorithm to search if there is a path from Roots[i] to Terminals[j];
        if such a path exists then
            Set the (i, j) entry of matrix B to 1;
        end
    end
end
if B is all-one matrix then
    return False;
otherwise do return True;
```

Proposition 4 *For a given static quantum circuit with n qubits and m operations, its reducibility can be efficiently determined by Algorithm 3 with time complexity of $O(mn^2)$.*

Proof Note that this approach combines three parts. First, we employ Algorithm 1 to derive the DAG representation of the given static circuit, which exhibits a time complexity of $O(m)$. Then, we convert the DAG to a simplified DAG by using DFS. For each root-terminal pair (r, t) in the DAG, DFS algorithm is applied to explore the existence of a path from r to t. Let $|R|$, $|T|$, $|V|$, and $|E|$ denote the number of roots, terminals, vertices, and edges in the DAG, respectively. It is clear that $|R| = |T| = n$, and $|V| = m$, $|E| = O(m)$ (each instruction introduces at most two edges to DAG). Since running DFS once in such a graph takes $O(|V| + |E|) = O(m)$ steps, and the number of trials we need is $|R| \times |T| = n^2$. So this part takes at most $O(mn^2)$ steps. Finally, after obtaining the reachability relation between all roots and terminals, we get the biadjacency matrix of the simplified DAG, which can be used to conclude the reducibility within n^2 steps.

Therefore, the overall time complexity required to determine the reducibility of a given static circuit is $O(m) + O(mn^2) + O(n^2)$, with the dominant term being $O(mn^2)$. ■

5.2 Approach 2: determine the reducibility from qubit reachability

It is worth noting that within the DAG representation of a quantum circuit, the connections between roots and terminals on distinct qubits are effectively established by vertices that correspond to double-qubit gates in the circuit. Capitalizing on this insight, we introduce the concept of qubit reachability within a quantum circuit and present our second approach to determine its reducibility.

Definition 5 (Reachability between qubits) *Given an instruction list of an n-qubit quantum circuit acting on the set of qubits $Q = \{q_0, q_1, \cdots, q_{n-1}\}$. Then any double-qubit instruction introduces two qubit relations*

$$q_i \xrightarrow{k} q_j \quad \text{and} \quad q_j \xrightarrow{k} q_i, \tag{3}$$

where q_i and q_j are the qubits upon which the instruction operates and k is the order index of the instruction within the instruction list. A qubit q_i reaches q_j (or, equivalently, q_j is reachable from q_i), denoted as $q_i \to q_j$, if there exists a sequence of qubit relations

$$q_i \xrightarrow{k_1} q_{l_1},\ q_{l_1} \xrightarrow{k_2} q_{l_2},\ \cdots,\ q_{l_s} \xrightarrow{k_{s+1}} q_j \tag{4}$$

such that $k_1 \le k_2 \le \cdots \le k_{s+1}$. Moreover, qubits q_i and q_j are mutually reachable if q_i reaches q_j and vice versa.

To illustrate this definition, consider the quantum circuit and its instructions in Figure 6. Here the order indices of each double-qubit instructions are the same as their IDs. For the first CNOT instruction acting on q_0 and q_1, it introduces two qubit relations $q_0 \xrightarrow{4} q_1$ and $q_1 \xrightarrow{4} q_0$. So we have $q_0 \to q_1$ and $q_1 \to q_0$, that is, they are mutually reachable. We can also see that $q_0 \to q_2$ because we have relation $q_0 \xrightarrow{4} q_1$ and $q_1 \xrightarrow{6} q_2$. But the reverse direction $q_2 \to q_0$ does not hold.

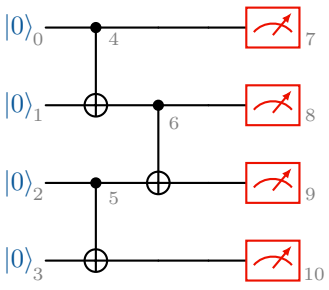

(a) Quantum circuit diagram.

Quantum Circuit Instructions

ID	TYPE	QUBIT	PAR
0	RESET	0	NONE
1	RESET	1	NONE
2	RESET	2	NONE
3	RESET	3	NONE
4	CX	[0, 1]	NONE
5	CX	[2, 3]	NONE
6	CX	[1, 2]	NONE
7	MEASURE	0	NONE
8	MEASURE	1	NONE
9	MEASURE	2	NONE
10	MEASURE	3	NONE

(b) Instructions for quantum circuit on the left.

Figure 6: An example of quantum circuit and its instructions.

The subsequent result demonstrates that qubit reachability constitutes a necessary and sufficient condition for determining circuit reducibility.

Proposition 6 *A static quantum circuit is irreducible if and only if any two qubits of this quantum circuit are mutually reachable.*

Proof Note that the sequence of qubit relations in Eq. (4) is equivalent to a subset of instructions involving interlacing qubits. This equivalence can further be represented as a directed path in the DAG representation, connecting the i-th root to the j-th terminal. Thus, any two qubits in the quantum circuit are mutually reachable if and only if a directed path exists in the DAG from any root to any terminal. This condition is equivalent to stating that the simplified DAG is complete. Finally, the proof is concluded by referring to Proposition 3. ■

The previous proof establishes the fundamental equivalence between qubit reachability and the connectivity of the simplified DAG, providing a valuable tool for determining the reducibility of a quantum circuit. However, as we will observe in Algorithm 4, the qubit reachability approach does not require the explicit construction of the DAG or the use of the DFS algorithm to derive the simplified DAG. Instead, we can establish qubit reachability by traversing the circuit instructions only once, progressively building up the reachability through a transitive rule.

For convenience, define the reachable set of q_i as the collection of all qubits that can reach q_i:

$$Q_i := \{q_j \in Q : q_j \to q_i\} \cup \{q_i\}. \tag{5}$$

This set is updated with each double-qubit instruction. For instance, in Figure 6, before the final CNOT instruction involving q_1 and q_2, the reachable sets are $Q_1 = \{q_0, q_1\}$ and $Q_2 = \{q_2, q_3\}$. Subsequently, after this instruction, any qubit in the set $Q_1 \cup Q_2 = \{q_0, q_1, q_2, q_3\}$ can reach both q_1 and q_2. So the reachable sets are updated to $Q_1 = \{q_0, q_1, q_2, q_3\}$ and $Q_2 = \{q_0, q_1, q_2, q_3\}$.

By harnessing this transitive rule, we can effectively determine circuit reducibility. The algorithm for this procedure is outlined in Algorithm 4, followed by an analysis of its time complexity in Proposition 7.

Algorithm 4: Determining reducibility from qubit reachability

Input:

StaticCircuit	the instruction list of a static quantum circuit

Output:

True or *False*	whether the static quantum circuit is reducible

```
Let n be the quantum circuit width;
Initialize a list ReachableSets of length n, with each element initialized as an empty set;
for i = 0 to n − 1 do add q_i to ReachableSets[i];
foreach Instruction in StaticCircuit do
    if Instruction is a double qubit gate then
        Record the QUBIT values of Instruction as i and j respectively;
        Calculate Union = ReachableSets[i] ∪ ReachableSets[j];
        Set ReachableSets[i] and ReachableSets[j] to Union;
    end
end
foreach ReachableSet in ReachableSets do
    if the length of ReachableSet is less than n then
        return Ture
    end
end
otherwise do return False;
```

Proposition 7 *For a given static quantum circuit with n qubits and m operations, its reducibility can be efficiently determined by Algorithm 4 with time complexity of $O(mn)$.*

Proof To determine the reducibility of a static circuit, it is necessary to analyze the reachability relation for each qubit. These reachability relations are stored in a list named the *ReachableSets*, which has a length of n, representing the circuit's width, with the i-th entry containing the reachable set Q_i. This initial process involves $O(n)$ steps. Subsequently, a 'foreach' loop is executed over the 'StaticCircuit' list, which comprises m elements. Throughout this loop, all operations, except the union set calculation, exhibit a constant time complexity of $O(1)$ as they are independent of the input size. However, the computational complexity for uniting two sets, S_1 and S_2, amounts to $O(|S_1| + |S_2|)$. It is worth noting that the reachable set of a qubit contains a maximum of n elements, thus the union calculation is bounded by $O(n)$. Consequently, the overall time complexity of the 'foreach' loop equates to $O(mn)$. In the final step, which determines reducibility, another 'foreach' loop is executed, iterating over the *ReachableSets*, incurring an additional $O(n)$ steps. In summary, the time complexity of Algorithm 4 is $O(mn) + O(n) + O(n)$, with the dominant factor remaining $O(mn)$. ■

5.3 Approach 3: determine the reducibility from matrix

The preceding approach by qubit reachability can be further formulated via Boolean matrix manipulation, which can be more convenient for analytical studies. Let $\mathcal{C}_1 \circ \mathcal{C}_2$ be a composition of quantum circuits $\mathcal{C}_1$ and $\mathcal{C}_2$ and let $B(\mathcal{C})$ be the biadjacency matrix of the simplified DAG of the quantum circuit $\mathcal{C}$. Then we have the following relation for quantum circuit composition.

Proposition 8 *Let $\mathcal{C}_1$ and $\mathcal{C}_2$ be two static quantum circuits. Then $B(\mathcal{C}_1 \circ \mathcal{C}_2) = B(\mathcal{C}_1) \odot B(\mathcal{C}_2)$.*

Proof Let G_m be the simplified DAG of circuit $\mathcal{C}_m$. Then the (i, j) entry of $B(\mathcal{C}_m)$ equals to one if and only if there is an edge from root r_i^m to terminal t_j^m in graph G_m. To study the simplified DAG of the composite circuit $\mathcal{C}_1 \circ \mathcal{C}_2$, we can connect all terminals t_k^1 in graph G_1 with their corresponding roots r_k^2 in graph G_2. Therefore, a path from r_i^1 to t_j^2 exists if and only if there is an edge from r_i^1 to t_k^1 in graph G_1, followed by an edge from r_k^2 to t_j^2 in graph G_2 for some intermediate k. This condition can be represented as $\vee_{k=1}^n (B(\mathcal{C}_1)_{ik} \wedge B(\mathcal{C}_2)_{kj})$, which is exactly the (i, j) entry of the Boolean matrix product $B(\mathcal{C}_1) \odot B(\mathcal{C}_2)$. ■

Note that if an n-qubit quantum circuit only contains one double-qubit gate, e.g., a CNOT gate acting on the i and j qubit, its biadjacency matrix is given by

$$B_{ij} = I_n + E_{ij}^n + E_{ji}^n, \tag{6}$$

where E_{ij}^n is the matrix whose (i, j) entry is one and zero otherwise. Since any quantum circuit can be seen as the composition of a sequence of subcircuits with only one double-qubit gate, then by Proposition 8 we can compute the biadjacency matrix of a quantum circuit as the product of a sequence of matrices of the form (6).

Remark 3 Consider a quantum circuit $\mathcal{C}$ comprising m double-qubit gates. Denote B_i as the biadjacency matrix of the subcircuits, each containing only a single double-qubit gate. Then the biadjacency matrix of $\mathcal{C}$ is given by $B = B_1 \cdots B_m$. Since $B_i^\top = B_i$, we get

$$B = (B_m B_{m-1} \cdots B_1)^T. \tag{7}$$

This corresponds to the concept of a dual circuit as presented in [DCKFF22]. In this context, we reverse the sequence of gates and exchange the roles of state preparation and measurement. The equality mentioned above implies that the dual circuit shares the same biadjacency matrix as the original circuit. Therefore, the compilation strategies for both circuits can be the same.

A more in-depth examination of the Boolean product reveals that there is no need to perform explicit matrix multiplication. More specifically, for any matrix A, we have

$$A \odot B_{ij} = (a_1, \cdots, a_i \vee a_j, \cdots, a_j \vee a_i, \cdots, a_n), \tag{8}$$

where a_i is the i-th column of the matrix A and $a_i \vee a_j$ represents entrywise OR of a_i and a_j. In other words, the impact of multiplying a matrix B_{ij} is equivalent to replacing the i-th and j-th columns of A with $a_i \vee a_j$. This gives the following algorithm for checking the reducibility of a quantum circuit.

Algorithm 5: Determining reducibility from matrix

Input:

StaticCircuit the instruction list of a static quantum circuit

Output:

True or *False* whether the static quantum circuit is reducible

```
Let n be the quantum circuit width;
Initialize B as an n × n identity matrix.;
foreach Instruction in StaticCircuit do
    if Instruction is a double-qubit gate then
        Record the QUBIT values of Instruction as i and j respectively;
        Calculate B' = B[i] ∨ B[j], where B[k] is the k-th column of matrix B;
        Set B[i] = B' and B[j] = B';
    end
end
if B is all-one matrix then
    return False;
otherwise do return True;
```

Proposition 9 *For a given static quantum circuit with n qubits and m operations, its reducibility can be efficiently determined by Algorithm 5 with time complexity of $O(mn)$.*

Proof First, a 'foreach' loop is executed over the *StaticCircuit* list, encompassing m elements. Throughout this loop, all operations, except for the calculation of the entrywise OR, exhibit a constant time complexity of $O(1)$, as they are independent of input size. Since each column of B contains n elements, the entrywise OR takes $O(n)$ steps. Consequently, the cumulative time complexity of the 'foreach' loop equates to $O(mn)$. The last part that determines if a Boolean matrix is all-one matrix takes $O(n^2)$ steps. In summary, the overall time complexity is $O(mn) + O(n^2)$, with the dominant factor remaining $O(mn)$ (typically, m is larger than n). ■

The following result explores the connection between the reducibility of a quantum circuit and its subcircuits.

Proposition 10 *A static quantum circuit is irreducible if it contains an irreducible subcircuit. The reverse direction is not true. That is, there exists an irreducible static quantum circuit such that any of its subcircuit is reducible.*

Proof Note that any quantum circuit $\mathcal{C}$ can be seen as a composition of a sequence of subcircuits with a single quantum gate $\mathcal{C} = \mathcal{C}_1 \circ \cdots \circ \mathcal{C}_M$. Let B_i be the biadjacency matrix of the simplified DAG of $\mathcal{C}_i$. The circuit $\mathcal{C}$ has an irreducible subcircuit implies that there exists $\mathcal{C}_{i_1} \circ \cdots \circ \mathcal{C}_{i_m}$ such that $\bigodot_{j=1}^{m} B_{i_j} = J$. Then this implies $\bigodot_{i=1}^{M} B_i \geq \bigodot_{j=1}^{m} B_{i_j} = J$, where the inequality signifies that each entry of the left matrix is greater than or equal to the corresponding entry in the right matrix. This proves the first statement. The quantum circuit in Figure 7 is an irreducible circuit with 4 qubits and 5 CNOTs. However, the removal of any CNOT in this circuit will result in a reducible circuit. ■

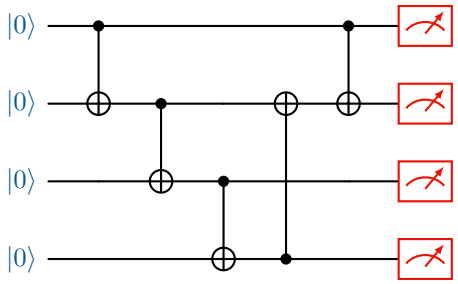

Figure 7: An irreducible static quantum circuit such that any of its subcircuit is reducible.

6 Optimal quantum circuit compilation

In this section, we introduce the mathematical model that characterizes optimal quantum circuit compilation. This model serves as the foundation for deriving heuristic algorithms and analyzing optimal compilation schemes for specific quantum circuits in the subsequent sections.

Proposition 11 *Finding the optimal dynamic circuit compilation scheme of a static quantum circuit with n qubits is equivalent to solving the following binary integer programming problem with n^2 Boolean variables F_{ij}:*

$$\alpha := \max \sum_{i,j=0}^{n-1} F_{ij} \tag{9a}$$

$$\text{s.t. } F_{ij} \leq \bar{B}_{ij},\ \forall i,j \in \{0,1,...,n-1\} \tag{9b}$$

$$\sum_{j=0}^{n-1} F_{ij} \leq 1,\ \forall i \in \{0,1,...,n-1\} \tag{9c}$$

$$\sum_{i=0}^{n-1} F_{ij} \leq 1,\ \forall j \in \{0,1,...,n-1\} \tag{9d}$$

$$\begin{pmatrix} O_n & B \\ F & O_n \end{pmatrix} \text{ nilpotent }, \tag{9e}$$

where B is the biadjacency matrix of the simplified DAG, $\bar{B} = \neg\,(B^\top)$, referred to as the candidate matrix, is the logical NOT of the transpose of matrix B. The block matrix in Eq. (9e) is the adjacency matrix of the modified DAG, which is used to compile the quantum circuit via Algorithm 2. Furthermore, the width of the compiled quantum circuit is given by $n - \alpha$.

Remark 4 It is worth noting that condition (9b) is indeed implied by condition (9e). However, we explicitly enforce this condition as it proves helpful in the analysis of the optimal solution for specific examples in Section 8. Furthermore, there are other equivalent variants of the optimization problem. For instance, the second condition can be omitted, allowing different terminals to connect to the same root. Nevertheless, this modification does not contribute to a reduction in the number of qubits. In such cases, the objective function should be adjusted accordingly.

Proof Let $G = (R, T, E)$ be the simplified DAG of the circuit and $R = \{r_0, ..., r_{n-1}\}$, $T = \{t_0, ..., t_{n-1}\}$. Then the adjacency matrix of the directed graph G, denoted as $A(G)$, is a $2n \times 2n$ block anti-diagonal matrix, where the first n rows/columns correspond to the n roots, and the last n rows/columns correspond to the n terminals. Since all edges in the original bipartite graph are

pointing from roots to terminals, only the $n \times n$ submatrix in the upper right corner has non-zero elements. Therefore, the adjacency matrix can be written in the form:

$$A(G) = \begin{pmatrix} O_n & B \\ O_n & O_n \end{pmatrix} \tag{10}$$

where B is the biadjacency matrix of the bipartite graph.

Note that the absence of directed edge from r_i to t_j in the original bipartite graph G indicates a candidate edge from t_j to r_i in the modified DAG. All these candidate edges are pointing from terminals to roots, therefore can be represented by the $n \times n$ submatrix $\bar{B}$ in the lower left corner of the adjacency matrix $A(G)$. The submatrix $\bar{B}$, can be obtained by:

$$\bar{B} = \neg (B^\top) \tag{11}$$

which is the logical NOT of the transpose of matrix B.

We use a $n \times n$ Boolean matrix F to represent all added edges, where the entry $F_{ij} = 1$ if a directed edge from t_i to r_j is added to the graph, and 0 otherwise. Suppose that G' is the modified DAG, then the adjacency matrix of G' can be written as:

$$A(G') = \begin{pmatrix} O_n & B \\ F & O_n \end{pmatrix} \tag{12}$$

The constraints imposed in Theorem 2 when adding edges to G can be translated into the following constraints on matrix F:

1. The objective of maximizing the number of added edges is equivalent to maximizing the sum of all elements in matrix F:

$$\max \sum_{i,j=0}^{n-1} F_{ij} \tag{13}$$

2. All added edges should be selected from candidate edges, which means elements of matrix F should be selected from elements of matrix $\bar{B}$ and can be expressed as:

$$F_{ij} \leq \bar{B}_{ij}, \forall i, j \in \{0, 1, ..., n-1\} \tag{14}$$

3. The added edges must not share common vertices, which implies the sum of each row/column of F can not exceed one:

$$\sum_{j=1}^{n} F_{ij} \leq 1, \forall i \in \{0, 1, ..., n-1\} \tag{15}$$

$$\sum_{i=1}^{n} F_{ij} \leq 1, \forall j \in \{0, 1, ..., n-1\}. \tag{16}$$

4. After incorporating these edges, the graph G' should remain acyclic. According to Lemma 1, this requirement is equivalent to the adjacency matrix of G' being nilpotent.

Finally, since the optimal value α gives the maximum number of terminal-root pairs in the modified DAG, the remaining number of roots is $n - \alpha$, which is the width of the compiled circuit. This completes the proof. ■

Remark 5 The difficulty in solving the binary integer programming problem presented in Proposition 11 arises from the presence of the nilpotent constraint. Due to the non-convex nature of the set of nilpotent matrices, the optimization problem in Proposition 11 is inherently non-convex.

7 Heuristic algorithms

The previous section demonstrated that the quantum circuit compilation problem is essentially a binary integer optimization problem with an exponentially increased solution space. While checking the reducibility of a quantum circuit is a polynomial-time task, as analyzed in Section 5, finding the optimal compilation scheme could potentially require exponential time. In this section, we introduce several efficient heuristic algorithms designed to address the optimization problem within polynomial time.

7.1 Algorithm 1: Minimum Remaining Values Heuristic

The Minimum Remaining Values (MRV) heuristic is a commonly employed technique in constraint satisfaction problems [RN09]. The concept underlying the MRV heuristic is to designate the variable with the fewest valid values (i.e., the minimum remaining values) as the next one for value assignment. This approach effectively narrows down the search space, leading to a more efficient problem-solving process. The MRV heuristic finds extensive application in practical problem-solving. For instance, in Sudoku Solvers, it involves selecting the empty cell with the fewest potential values for the next value assignment. Likewise, in the context of the Map Coloring Problem, the MRV heuristic guides the choice of a country with the fewest uncolored neighboring countries as the next candidate for coloring. In a broader context, the MRV heuristic can be employed in any constraint satisfaction problem where the objective is to systematically find a solution by systematically assigning values to variables.

In the context of our dynamic circuit compilation problem, we can implement the MRV heuristic algorithm as follows. Consider a 5-qubit Bernstein–Vazirani algorithm, with its biadjacency matrix B provided in Figure 8(a), and the candidate matrix $\bar{B} = \neg (B^\top)$ given in Figure 8(b). Let's assume that the rows and columns are indexed by $\{t_0, \cdots, t_4\}$ and $\{r_0, \cdots, r_4\}$. During each iteration, we first identify the terminal t_i with the fewest candidate roots according to the candidate matrix and connect it to a candidate root r_j with the least number of choices of terminals. In this example, the candidate edge is selected as (t_3, r_1), as depicted in green. After adding this edge, we need to update the candidate matrix. Prior to the incorporation of this edge, the set R_i encompasses all roots capable of reaching terminal t_i, while the set T_j represents all terminals that are reachable from root r_j. In this example, we have $R_1 = \{r_0, r_2, r_3, r_4\}$ and $T_3 = \{t_1\}$. Upon adding this edge, any root r in the set R_i will gain the ability to reach any terminal t in the set T_j, which indicates that all edges (t, r) where $t \in T_j$ and $r \in R_i$ are no longer candidate edges. Consequently, we need to update all these entries in the candidate matrix to zero. That is, set entries $(t_1, r_0), (t_1, r_2), (t_1, r_3), (t_1, r_4)$ to zero, which is depicted in Figure 8(c). Furthermore, to ensure that the added edges do not share common vertices, it is necessary to update all entries in the t_i row and all entries in the r_j column of the candidate matrix to zero. In this example, set all entries in the t_3 row and all entries in the r_1 column to zero, which is depicted in Figure 8(d).

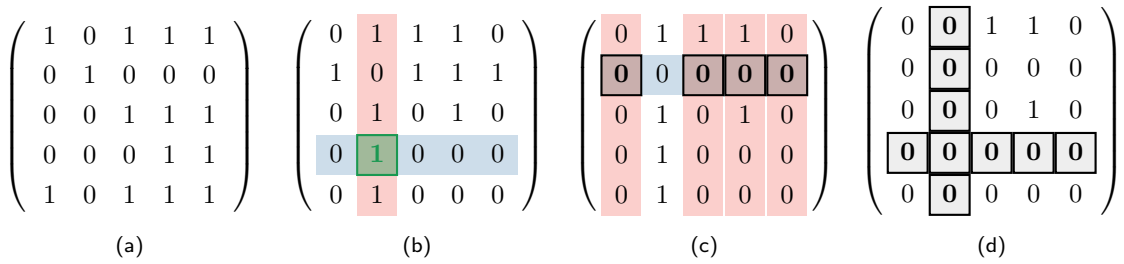

Figure 8: An illustration of MRV heuristic algorithm. Suppose the row and column of the matrix are indexed by $\{t_0, \cdots, t_4\}$ and $\{r_0, \cdots, r_4\}$. (a) the biadjacency matrix B of the simplified DAG of a 5-qubit Bernstein–Vazirani algorithm; (b) the candidate matrix $\bar{B} = \neg (B^\top)$ whereas the candidate edge is chosen as (t_3, r_1) marked in green; (c) set all entries in $T_3 \times R_1$ to zero , where $T_3 = \{t_1\}$ and $R_1 = \{r_0, r_2, r_3, r_4\}$; (d) set all entries in the t_3 row and all entries in the r_1 column to zero.

The complete MRV algorithm is given in Algorithm 6.

Algorithm 6: MRV heuristic algorithm

Input:

StaticCircuit the instruction list of a static quantum circuit to compile

Output:

DynamicCircuit the instruction list of the compiled dynamic quantum circuit

Run Algorithm 1 to get the DAG representation *Digraph* of the circuit;
Let *Roots* and *Terminals* be the set of roots and terminals, respectively;
Run Algorithm 5 to get the biadjacency matrix B of the simplified DAG of the circuit;
Calculate the candidate matrix *CandidateMatrix* as $\neg(B^\top)$;
Initialize two empty lists *CandidatesNum* and *AddedEdges*;
while *CandidateMatrix is not zero matrix* **do**
    Calculate the sum of each row of *CandidateMatrix* and record it in *CandidatesNum*;
    Identify the smallest non-zero element in *CandidatesNum* and record its index as t;
    Identify the non-zero element in the t-th row of *CandidateMatrix* with the smallest column sum and record its column index as r;
    Append the edge (*Terminals*[t], *Roots*[r]) to *AddedEdges*;
    Let R be the column indices of zero elements in the t-th row of *CandidateMatrix*;
    Let T be the row indices of zero elements in the r-th column of *CandidateMatrix*;
    foreach *pair* (u, v) *where* $u \in T$ *and* $v \in R$ **do**
        Set the entry (u, v) of *CandidateMatrix* to zero;
    end
    Set all entries in the t-th row and the r-th column of *CandidateMatrix* to zero;
end
Add *AddedEdges* to *Digraph* and get the *ModifiedGraph*;
Run Algorithm 2 to get the compiled circuit *DynamicCircuit*;
return *DynamicCircuit*

Remark 6 Note that the role of root and terminal in Algorithm 6 can be swapped. That is, we can identify the root with the fewest candidate terminals and connect it to a candidate terminal with least choice of roots. In practice, we can run both algorithms and then choose the result that yields a more optimal compilation.

Proposition 12 *For a static quantum circuit with n qubits and m operations, Algorithm 6 has a worst case time complexity of $O(mn + n^3)$.*

Proof The MRV heuristic algorithm comprises three key steps. Initially, Algorithm 1 and Algorithm 5 are applied to derive the DAG and the biadjacency matrix of the simplified DAG of the input static circuit and calculate the candidate matrix, which exhibits a time complexity of $O(m) + O(mn) + O(n^2) = O(mn)$. Subsequently, our MRV heuristic is applied on the candidate matrix of size $n \times n$ to explore a feasible assignment. Since the maximum number of added edges is $n-1$, the 'while' loop iterates at most $n-1$ times. Within the loop, several operations are adapted to identify a candidate edge, where the row summation of the candidate matrix takes $O(n^2)$ time, the candidate terminal identification takes $O(n)$ times, while the candidate root identification involves traversing all candidate roots and summing of the corresponding columns, resulting in a worst-case time complexity of $O(n^2)$. Following this, the candidate matrix needs to be updated. Given that sets R and T contain a maximum of $n-1$ elements, this encompasses the update of at most $(n-1)^2$ entries, which can be completed in $O(n^2)$ time. Consequently, the time complexity of the entire 'while' loop is $O(n^3) + O(n^2) + O(n^3) + O(n^3) = O(n^3)$. Upon obtaining a list of added edges, Algorithm 2 is employed to compile the input static circuit, which requires $O(mn)$

time. In summary, the total time complexity of the MRV heuristic algorithm is calculated as: $O(mn) + O(n^3) + O(mn) = O(mn + n^3)$. ■

7.2 Algorithm 2: Greedy Heuristic Algorithm

Greedy algorithms are time-efficient heuristic strategy that makes a locally optimal choice at each step. This idea can be readily applied to address the dynamic circuit compilation problem as follows: in each iteration, the algorithm evaluates the potential impact of adding each candidate edge and selects the one that maximizes the possibility to add more edges in subsequent steps. Specifically, for each candidate edge, the algorithm temporarily integrates this edge into the simplified DAG and updates the candidate matrix following the rules outlined in Algorithm 6. The summation of all elements within the updated candidate matrix serves as the score for the candidate edge, which is then stored in the corresponding entry in a matrix called the *score matrix*. After evaluating all candidate edges, the algorithm identifies the candidate edge with the highest score as the optimal choice for inclusion in the current iteration and updates the candidate matrix accordingly before proceeding to the next iteration. In cases where multiple entries share the highest score, one edge is randomly selected from among them. An illustrative example of the scoring procedure is depicted in Figure 9.

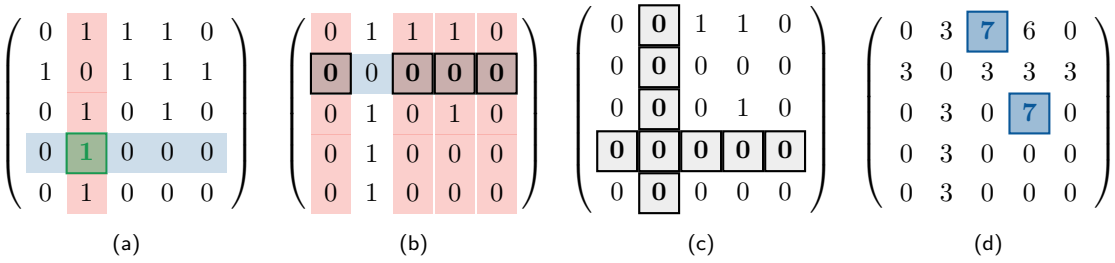

Figure 9: An illustration of the greedy heuristic algorithm. Suppose the row and column of the matrix are indexed by $\{t_0, \cdots, t_4\}$ and $\{r_0, \cdots, r_4\}$. (a) the candidate matrix of the simplified DAG of a 5-qubit Bernstein–Vazirani algorithm $\bar{B} = \neg (B^\top)$ whereas the candidate edge under evaluation is (t_3, r_1) marked in green; (b) set all entries in $T_3 \times R_1$ to zero , where $T_3 = \{t_1\}$ and $R_1 = \{r_0, r_2, r_3, r_4\}$; (c) set all entries in the t_3 row and all entries in the r_1 column to zero, the summation of all elements in the updated candidate matrix serves as the score of the candidate edge (t_3, r_1); (d) the score matrix after the first iteration, where the edge for inclusion in this round is randomly selected from the entries with the highest score (marked in blue).

The complete greedy algorithm is given in Algorithm 7.

Remark 7 The scoring rule in the greedy algorithm can be substituted with alternative approaches. For instance, the first three constraints described in Proposition 11 are equivalent to finding the maximum matching in a bipartite graph. Consequently, a viable alternative is to utilize the cardinality of the maximum matching within the updated candidate matrix as a metric for scoring each candidate edge.

Remark 8 In cases where multiple candidate edges share the highest score within a single round, a straightforward strategy is to select the one with the smallest entry index. However, it's important to note that any permutation of the qubit indices would result in a change in the entry index for a given edge. This makes the deterministic procedure dependent on the specific qubit labels and may limit the algorithm's performance. To mitigate this limitation, the introduction of a random selection process becomes essential. By running the algorithm multiple times, this stochastic approach has the potential to discover improved solutions, which we found to be quite useful in our numerical experiments.

Algorithm 7: Greedy heuristic algorithm

Input:

StaticCircuit the instruction list of a static quantum circuit to compile

Output:

DynamicCircuit the instruction list of the compiled dynamic quantum circuit

Run Algorithm 1 to get the DAG representation *Digraph* of the circuit;
Let *Roots* and *Terminals* be the set of roots and terminals, respectively;
Run Algorithm 5 to get the biadjacency matrix B of the simplified DAG of the circuit;
Calculate the candidate matrix *CandidateMatrix* as $\neg(B^\top)$;
Initialize an empty list *AddedEdges*;
while *CandidateMatrix is not zero matrix* **do**
    Initialize a $n \times n$ zero matrix *ScoresMatrix*;
    foreach *non-zero entry* (i, j) *in CandidateMatrix* **do**
        Initialize a matrix $\bar{B}_{i,j}$ as *CandidateMatrix*;
        Let R_i be the column indices of zero elements in the i-th row of $\bar{B}_{i,j}$;
        Let T_j be the row indices of zero elements in the j-th column of $\bar{B}_{i,j}$;
        foreach *pair* (u, v) *where* $u \in T_j$ *and* $v \in R_i$ **do**
            Set the entry (u, v) of $\bar{B}_{i,j}$ to zero;
        end
        Set all entries in the i-th row and all entries in the j-th column of $\bar{B}_{i,j}$ to zero;
        Set the entry (i, j) in *ScoresMatrix* to the sum of all entries in $\bar{B}_{i,j}$ plus one;
    end
    Identify all entries with the largest score in *ScoresMatrix* as *MaxScore*;
    Randomly select one entry in *MaxScore* and record its index (t, r);
    Append the edge (*Terminals*$[t]$, *Roots*$[r]$) to *AddedEdges*;
    Update *CandidateMatrix* to $\bar{B}_{t,r}$
end
Add *AddedEdges* to *Digraph* and get the *ModifiedGraph*;
Run Algorithm 2 to get the compiled circuit *DynamicCircuit*;
return *DynamicCircuit*

Proposition 13 *For a static quantum circuit with n qubits and m operations, Algorithm 7 has a worst case time complexity of $O(mn + n^5)$.*

Proof Similar to the MRV heuristic algorithm, both the initial step to get the candidate matrix and the final step to compile the input static circuit has a time complexity of $O(mn)$, while the primary 'while' loop iterates at most $n-1$ times. However, the main difference between the greedy heuristic and the MRV heuristic lies in the candidate edge identification process. In the worst-case scenario, where the biadjacency matrix is an identity matrix and the candidate matrix has (n^2-n) non-zero entries. Each of these entries triggers the update of the candidate matrix and the summation of a matrix's elements, which both exhibit a time complexity of $O(n^2)$. As a result, the total time complexity of the scoring step becomes $O(n^4)$. Subsequently, both the identification of the entry with maximum scoring and the corresponding candidate matrix update can be completed within $O(n^2)$ time. In summary, the total time complexity of the greedy heuristic algorithm 7 is evaluated as $O(mn) + O(n^5) + O(n^3)$, with the dominating term being $O(mn) + O(n^5)$. ■

7.3 Algorithm 3: Hybrid Algorithm

To further enhance the performance of the MRV algorithm, we introduce a hybrid algorithm by combining the MRV heuristic and brute force search. Initially, the hybrid algorithm employs a brute force search on a designated subset of terminals, denoted as $T_E \subseteq T$, which exhaustively enumerates all feasible edge additions pertinent to terminals within this subset. Subsequently, the MRV heuristic algorithm is employed to identify edges that can be added to the remaining terminals in $T - T_E$. Let L denote the cardinality of the subset $L = |T_E|$. Notably, at $L = 0$ the hybrid algorithm aligns precisely with the the MRV algorithm. As L increases, the hybrid algorithm progressively approximates the characteristics of the brute force search. Upon reaching $L = n$, the hybrid algorithm becomes the brute force search. This hierarchical variation of the hybrid algorithm, characterized by different values of L, which we referred as *the hierarchy level*, provides the opportunity to trade-off between the quality of the solution and the computational time complexity. The complete algorithm with hierarchy level L is shown in Algorithm 8.

Given that the search space is the Cartesian product of candidate roots sets of all terminals in T_E, the algorithm initiates by identifying L terminals with the least number of candidate roots, which significantly contracts the search space. Note that for each $t \in T_E$, we add a $\perp$ to the set of candidate roots to represent the situation where t connects no root. Due to the constraint that each terminal can be connected to only one root, solutions with repeated items (except $\perp$) in the calculated search space are rendered unfeasible and are consequently eliminated. Subsequently for each feasible solution, we check whether the DAG with these additional edges is acyclic. Once acyclicity is verified, Algorithm 3 is employed on the modified DAG to update the candidate matrix for the remaining terminals and roots, followed by Algorithm 6 to identify the further added edges. Finally, the solution featuring the highest number of added edges is selected to compile the input static circuit.

Algorithm 8: Hybrid algorithm with hierarchy level L

Input:

L	the hierarchy level
StaticCircuit	the instruction list of a static quantum circuit to compile

Output:

DynamicCircuit	the instruction list of the compiled dynamic quantum circuit

```
Run Algorithm 1 to get the DAG representation Digraph of the circuit;
Let Roots and Terminals be the set of roots and terminals, respectively;
Run Algorithm 5 to get the biadjacency matrix B of the simplified DAG of the circuit;
Calculate the candidate matrix CandidateMatrix as ¬(B^⊤);
Initialize empty lists MaxEdges, CandidatesNum, IdxTerminals, IdxRoots and SearchSpace;
Let CandidatesNum be the sum of each row in CandidateMatrix;
Let IdxTerminals be indices of the first L smallest non-zero values in CandidatesNum;
foreach Index in IdxTerminals do
    Let R be indices of non-zero entries in the Index-th row of CandidateMatrix;
    Add an element ⊥ to R, and append R to IdxRoots;
end
Calculate the Cartesian product of sets in IdxRoots and record it in SearchSpace;
Delete any elements with repeated items (except ⊥) from SearchSpace;
foreach Solution in SearchSpace do
    Initialize an empty list AddedEdges;
    for i = 0 to L − 1 do
        if Solution[i] is not ⊥ then
            Add edge (Terminals[IdxTerminal[i]], Roots[Solution[i]]) to AddedEdges;
        end
    end
    if Digraph with AddedEdges is acyclic then
        Run Algorithm 3 with Digraph and AddedEdges to get a updated simplified DAG
          and then the updated candidate matrix CanSubMatrix;
        Run Algorithm 6 with CanSubMatrix to get the added edges Edges;
        Append Edges to AddedEdges;
        if the length of AddedEdges is larger than the length of MaxEdges then
            Set MaxEdges to AddedEdges;
        end
    end
end
Add MaxEdges to Digraph and get the ModifiedGraph;
Run Algorithm 2 with the ModifiedGraph to get the compiled circuit DynamicCircuit;
return DynamciCircuit
```

Proposition 14 *For a static quantum circuit with n qubits and m operations, Algorithm 8 with hierarchy level L has a worst case time complexity of $O(n^L m^2 (n-L)^2)$.*

Proof The primary complexity of this algorithm arises from the enumeration process (the second 'foreach' loop). In the worst case, each terminal $t \in T_E$ has $(n-1)$ candidate roots, leading to a search space of size at most $(n-1)^L$. Within the search space, each solution undergoes a topological sorting to check whether DAG with additional edges is acyclic. This operation leverages the DFS algorithm, which carries a time complexity of $O(m)$. Following the topological sorting step, Algorithm 3 is executed on the modified DAG to update both the simplified DAG and the candidate matrix of the remaining $(n-L)$ terminals and roots, which demands $O(m(n-L)^2)$

time as outlined in Proposition 4. Subsequently, the MRV heuristic algorithm is employed to identify edges can be added between the remaining terminals and roots. Proposition 12 indicates that the MRV algorithm operating on a $(n-L)\times(n-L)$ candidate matrix exhibits a worst case time complexity of $O(m(n-L)+(n-L)^3)$. Consequently, the total time complexity of the hybrid algorithm is given by: $O(n^L m^2(n-L)^2)+O(n^L m^2(n-L))+O(n^L m(n-L)^3)$, where the dominant factor is $O(n^L m^2(n-L)^2)$ since m is typically larger than n. ■

8 Examples

In this section, we conduct a thorough analysis of quantum circuits with practical relevance, offering optimal compilations for well-known quantum algorithms in quantum computation, ansatz circuits utilized in quantum machine learning, and measurement-based quantum computation crucial for quantum networking. We also perform a comparative analysis against state-of-the-art approaches, demonstrating the superior performance of our methods in both structured and random quantum circuits. A brief summary of the quantum circuits explored in this study is provided in Table 2.

Quantum circuits	Original width	Compiled width	Reference
Deutsch-Jozsa algorithm	n	2 (1)	Proposition 15
Bernstein-Vazirani algorithm	n	2 (1)	Proposition 16
Simon's algorithm	$2n$	3	Proposition 17
Quantum Fourier transform	n	n	Section 8.1.4
Quantum phase estimation	n	n	Section 8.1.5
Shor's algorithm	n	n	Section 8.1.6
Grover's algorithm	n	n	Section 8.1.7
Quantum counting algorithm	n	n	Section 8.1.8
Linearly entangled circuit with l layers	n	$l+1$	Proposition 18
Circularly entangled circuit with l layers	n	3	Proposition 19
Pairwisely entangled circuit with l layers	n	$2l+1$	Proposition 20
Fully entangled circuit	n	n	Proposition 21
Diamond-structured quantum circuit	$2n$	$n+1$	Proposition 22
MBQC with cluster state of size (w,d)	wd	$w+1$	Proposition 23
MBQC with brickwork state of size (w,d)	wd	$w+1$	Remark 9
Quantum ripple carry adder circuit	n (4)	4 (3)	Proposition 24
Quantum supremacy circuits	-	-	Section 8.4
GRCS circuits	-	-	Section 8.4
QAOA circuits for max-cut	-	-	Section 8.5

Table 2: A summary of the quantum circuits studied in this work. The case in blue indicates irreducible circuits, while the case in red means the compiled width is optimal. Numerical studies are provided for cases in green.

8.1 Frequently used quantum algorithms

8.1.1 Deutsch-Jozsa algorithm

The Deutsch-Jozsa algorithm [DJ92] was the pioneering example of a quantum algorithm that outperforms classical counterparts. It exemplifies the advantages of using quantum computing for specific problems. The algorithm's objective is to determine the nature of a Boolean function $f:\{0,1\}^n\to\{0,1\}$—whether it is balanced or constant. This algorithm is represented by the following $(n+1)$-qubit quantum circuit. The initial state has the first n qubits set to $|0\rangle$, and the last qubit initialized as $|1\rangle = X|0\rangle$. A Hadamard gate is subsequently applied to each qubit. Following this, a quantum oracle U_f maps $|x\rangle|y\rangle$ to $|x\rangle|y\oplus f(x)\rangle$. Finally, Hadamard gates are reapplied to the first n qubits, and they are measured in the computational basis.

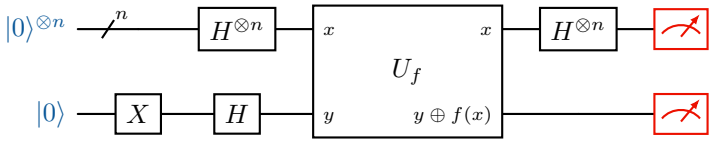

Figure 10: The Deutsch-Jozsa algorithm for determing an n-bit Boolean function.

If the Boolean function f is constant, the quantum oracle U_f can be implemented using only single-qubit gates, making it trivially reducible to a quantum circuit with 1 qubit. In the case where the Boolean function f is balanced, multiple quantum circuit implementations are possible. For instance, the quantum oracle U_f can be realized using a quantum circuit depicted in Figure 11, that is, regardless of the single-qubit gates, applying a CNOT gate for each of the first n qubits, with the $(n+1)$-th qubit as the target.

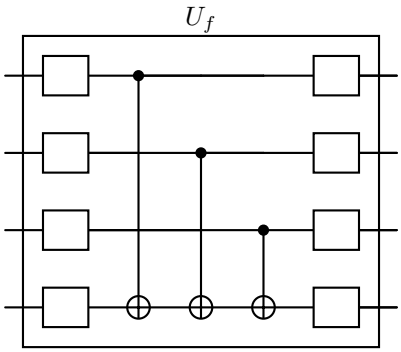

Figure 11: A quantum circuit implementation of a balanced oracle for determining a 3-bit Boolean function. The empty box represents a single-qubit gate.

The following result gives an optimal compilation of the Deutsch-Jozsa algorithm.

Proposition 15 (Deutsch-Jozsa.) *The quantum circuit of the Deutsch-Jozsa algorithm for determining an n-bit Boolean function f contains $n+1$ qubits ($n \geq 2$). This circuit is always reducible. If f is constant, the quantum circuit can be reduced to a dynamic quantum circuit with 1 qubit. Otherwise, it can be reduced to a dynamic quantum circuit with 2 qubits. In this case, the corresponding optimal solution for optimization (9) can be taken at $\sum_{i=0}^{n-2} E_{i,i+1}^{n+1}$.*

Proof If the function is constant, the quantum circuit only contains single-qubit gate. So it can be trivially reduced to a quantum circuit with 1. Now we prove the other case. For the quantum circuit implementation in Figure 11, the biadjacency matrix of the simplified DAG is given by

$$B = \sum_{i=0}^{n} \sum_{j=i}^{n} E_{i,j}^{n+1} + \sum_{i=0}^{n-1} E_{n,i}^{n+1}. \tag{17}$$

So the candidate matrix is

$$C = \sum_{i=0}^{n-2} \sum_{j=i+1}^{n-1} E_{i,j}^{n+1}. \tag{18}$$

For the optimal compilation, we need to select the maximum number of 1 elements in such a matrix under the conditions stated in Proposition 11. Without the nilpotent condition, the maximum number of 1 elements that simultaneously satisfies conditions (9b), (9c) and (9d) is $n-1$. Let us choose

$$F = \sum_{i=0}^{n-2} E_{i,i+1}^{n+1}, \tag{19}$$

with the total sum of $n-1$. Then we can easily check that the adjacency matrix with such a selection is indeed nilpotent, making it an optimal solution in (9). Finally, by Algorithm 2, the compiled circuit has a circuit width 2. ■

8.1.2 Bernstein-Vazirani algorithm

The Bernstein-Vazirani algorithm [BV97] can be considered an extension of the Deutsch-Jozsa algorithm, demonstrating the advantages of using a quantum computer as a computational tool for more complex problems than the Deutsch-Jozsa problem. Instead of distinguishing between two different classes of functions, it is designed to recover a string encoded within a function. Specifically, when provided with an oracle implementing a function $f : \{0,1\}^n \to \{0,1\}$ in which $f(x)$ is promised to be the dot product between x and a secret string $s \in \{0,1\}^n$ modulo 2, the objective is to determine the value of s. The Bernstein-Vazirani algorithm employs the same $(n+1)$-qubit quantum circuit as depicted in Figure 10. Furthermore, the quantum oracle can be realized by applying a CNOT gate to the corresponding qubit with the last qubit as the target for each bit in the string s that equals one. For example, if the bit string is $s = 101$, the quantum oracle is implemented as

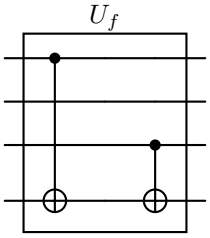

Figure 12: A quantum circuit implementation of an oracle for $f(x) = (x_0 + x_2) \mod 2$.

The following result gives an optimal compilation of the Bernstein-Vazirani algorithm.

Proposition 16 (Bernstein-Vazirani.) *The quantum circuit of the Bernstein-Vazirani algorithm for determining an n-bit Boolean function f contains $n+1$ qubits ($n \geq 2$). This circuit is always reducible. If f is constant, the quantum circuit can be reduced to a dynamic quantum circuit with 1 qubit. Otherwise, it can be reduced to a dynamic quantum circuit with 2 qubits. In this case, the corresponding optimal solution for optimization (9) can be taken at $\sum_{i=0}^{n-2} E_{i,i+1}^{n+1}$.*

Proof If the secret string is all zero, then the function is constant and the quantum oracle contains no multi-qubit gates. This makes the circuit trivially reducible to one qubit. Otherwise, the secret string contains at least one non-zero element. So the quantum oracle has at least one CNOT gate. Without loss of generality, we can consider the case in which the secret string is all one. This is because the quantum circuit for all the other cases is a subcircuit of this one. In this case, the quantum circuit structure is the same as the Deutsch-Jozsa algorithm when omitting the single-qubit gates. So the rest of proof follows exactly the same as the proof of Proposition 15. ■

8.1.3 Simon's algorithm

Simon's algorithm [Sim97] marked a significant milestone as the first quantum algorithm to exhibit an exponential speed-up when compared to the best classical algorithm for a specific problem. This breakthrough served as a foundational inspiration for a family of quantum algorithms centered around the quantum Fourier transform, including the renowned Shor's factoring algorithm. In the problem Simon's algorithm addresses, we are provided with an oracle that is guaranteed to have either a one-to-one mapping (it maps a unique output to every input) or a two-to-one mapping (it maps two different inputs to a single unique output). The nature of this two-to-one mapping is determined by a secret bitstring s, where the function $f(x)$ equals $f(y)$ if and only if $y = x \oplus s$. The primary objectives are twofold: first, to decide whether the function f is one-to-one or two-to-one;

and second, in the event it is determined to be two-to-one, to unveil the secret bitstring s. The quantum circuit implementation of Simon's algorithm is given by

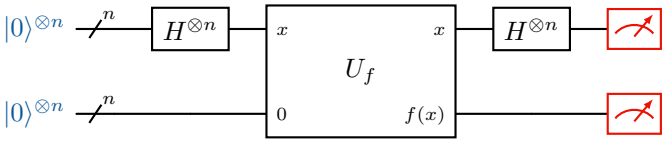

Figure 13: The Simon's algorithm for determining an n-bit Boolean function.

There are many possible ways of implementing a desired two-to-one function. Here we can consider a specific choice that

$$f(x) = \begin{cases} x, & x_j = 0, \\ x \oplus s, & x_j = 1, \end{cases} \tag{20}$$

where x_j is the j-th bit of x and j is the smallest index where the bit of s equals to one. For example, if $s = 011$, then $j = 1$. In this case, the quantum oracle U_f can be implemented by first performing a CNOT gate between i-th and $n+i$-th qubits for every $i \in \{0, 1, \cdots, n-1\}$ and then performing a CNOT gate on the j-th qubit and the $n+k$-th qubit whenever the k-th bit of s equals to one. For instance, given secret string $s = 011$, the quantum oracle U_f can be implemented by

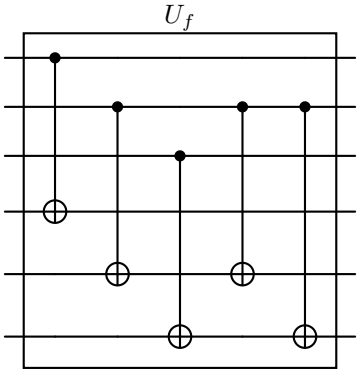

Figure 14: A quantum circuit implementation of an oracle for secret string $s = 011$.

Proposition 17 (Simon.) *The quantum circuit of the Simon's algorithm for determining an n-bit function f contains $2n$ qubits ($n \geq 2$). This circuit is always reducible. It can be reduced to a dynamic quantum circuit with 3 qubits. In this case, the corresponding optimal solution for optimization (9) can be taken at $E^2_{0,0} \otimes \sum_{i=1}^{n-2} E^n_{i,i+1} + E^2_{1,1} \otimes \sum_{i=0}^{n-2} E^n_{i,i+1}$.*

Proof Note that any quantum circuit is a subcircuit of the one given by a secret string with all-one values. So we can restrict our consideration in the later case, where a CNOT is applied between i-th and $i+n$-th qubits for every $i \in \{0, 1, \cdots, n-1\}$ and a CNOT is applied between 0-th and $i+n$-th qubits for every $i \in \{0, 1, \cdots, n-1\}$. In this case, the biadjacency matrix of the simplified DAG is given by

$$B = (E^2_{0,0} + E^2_{1,0}) \otimes \left(I_n + \sum_{i=1}^{n-1} E^n_{i,0} \right) + (E^2_{0,1} + E^2_{1,1}) \otimes \sum_{i=0}^{n-1} \sum_{j=i}^{n-1} E^n_{i,j}. \tag{21}$$

So the candidate matrix is

$$C = (E^2_{0,0} + E^2_{0,1}) \otimes \left(\sum_{i=1}^{n-2} \sum_{j=i+1}^{n-1} E^n_{i,j} + \sum_{i=1}^{n-1} \sum_{j=0}^{i-1} E^n_{i,j} \right) + (E^2_{1,0} + E^2_{1,1}) \otimes \sum_{i=0}^{n-2} \sum_{j=i+1}^{n-1} E^n_{i,j}. \tag{22}$$

Without the nilpotent condition, we can choose

$$F = E^2_{0,0} \otimes \sum_{i=1}^{n-2} E^n_{i,i+1} + E^2_{1,1} \otimes \sum_{i=0}^{n-2} E^n_{i,i+1}, \tag{23}$$

with the total sum of $2n-3$. Then we can easily check that the adjacency matrix with such a selection is indeed nilpotent, making it a feasible solution in (9). Finally, by Algorithm 2, the compiled circuit has circuit width 3. Note that if we take $n = 2$, the quantum circuit is a subcircuit for any quantum circuit with larger n. In the case of $n = 2$, we can easily enumerate all possible compilation schemes and conclude that it requires at least 3 qubits in the compiled quantum circuit. This implies that any larger circuit will also require at least 3 qubits and concludes the optimality of our feasible solution in (23). ■

8.1.4 Quantum Fourier transform

The Fourier transform is a fundamental concept in classical computing with various applications, including signal processing, data compression, and complexity theory. In quantum computing, the quantum Fourier transform (QFT) serves as the quantum analog of the discrete Fourier transform and operates on the amplitudes of a quantum wavefunction. The QFT plays a pivotal role in numerous quantum algorithms, with its most notable appearances in Shor's factoring algorithm and quantum phase estimation. The quantum Fourier transform acts on a quantum state $|x\rangle = \sum_{j=0}^{2^n-1} x_j|j\rangle$ and maps it to another quantum state $|y\rangle = \sum_{k=0}^{2^n-1} y_k|k\rangle$ where $y_k = \frac{1}{\sqrt{2^n}} \sum_{j=0}^{2^n-1} x_j e^{2\pi ijk/2^n}$. Let $R_k = |0\rangle\langle 0| + e^{2\pi i/2^k}|1\rangle\langle 1|$. Then the quantum Fourier transform can be implemented by the following quantum circuit. For every $j \in \{0, 1, \cdots, n-1\}$, apply a Hadamard gate on the j-th qubit and then apply a controlled-R_k gate between the j-th qubit and the $(j+k-1)$-th qubit for every $k \in \{2, \cdots, n-j\}$. Finally, apply SWAP gates to reverse the order of the qubits. For instance, the quantum circuit for $n = 4$ is illustrated below.

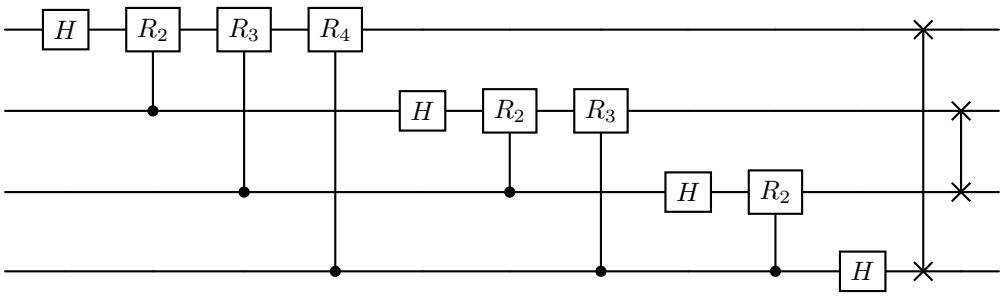

Figure 15: A quantum circuit implementation of the quantum Fourier transform for $n = 4$.

Since there is a double-qubit gate on any two qubits in the quantum circuit of the quantum Fourier transform, this quantum circuit is clearly irreducible by Proposition 6.

8.1.5 Quantum phase estimation

The Fourier transform plays a crucial role in a general procedure known as phase estimation, which serves as a fundamental component in many quantum algorithms. Consider a unitary operator U that possesses an eigenvector $|u\rangle$ with an associated eigenvalue of $e^{2\pi i\theta}$, where the precise value of θ remains unknown. The objective of the phase estimation algorithm is to estimate the value of θ. To conduct this estimation, we assume the availability of oracles capable of preparing the state $|u\rangle$ and performing controlled-U^{2^j} operations, with j being a non-negative integer. The quantum phase estimation procedure involves two registers. The first register comprises t qubits, initially set to $|0\rangle$. The choice of the value of t depends on two factors: the level of precision required for estimating θ, and the desired probability of a successful phase estimation procedure. The second register begins in the state $|u\rangle$ and accommodates a number of qubits sufficient to store $|u\rangle$. Phase

estimation unfolds in two stages. First, the circuit commences by applying a Hadamard transform to the first register, followed by a series of controlled-U operations on the second register, each involving U raised to successive powers of two. The second stage of phase estimation involves the application of the inverse quantum Fourier transform. An example is provided in Figure 16.

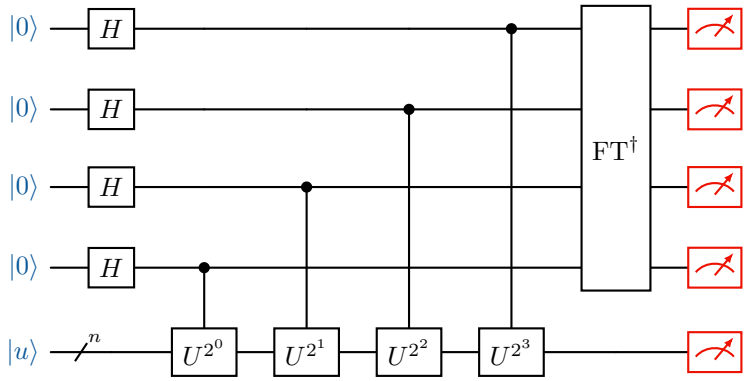

Figure 16: A quantum circuit implementation of the quantum phase estimation for $t = 4$.

The original quantum circuit for quantum phase estimation necessitates the utilization of $t+n$ qubits. It is important to observe that the reducibility of a quantum circuit is equivalent to the reducibility of its dual circuit, which is essentially the circuit with a reversed gate sequence. In the context of the phase estimation algorithm, the dual circuit is structured as follows: it begins with the quantum Fourier transform applied to the first t qubits, followed by a sequence of controlled-U operations conducted on each qubit within the initial t qubits and the subsequent n qubits. The quantum Fourier transform gives the biadjacency matrix as

$$B_{-1} = \begin{pmatrix} J_t & O \\ O & I_n \end{pmatrix} \tag{24}$$

For every controlled operation acting on the k-th qubit and the last n qubits, the biadjacency matrix is given by

$$B_k = I_{t+n} + \sum_{\substack{i \neq j \\ i,j \in \{k,t,t+1,\cdots,t+n-1\}}} (E_{i,j}^{t+n} + E_{j,i}^{t+n}). \tag{25}$$

According to Proposition 8, the biadjacency matrix for the dual circuit of quantum phase estimation is given by

$$B_{-1} \odot \left(\bigodot_{k=0}^{t-1} B_k \right), \tag{26}$$

which is an all-one matrix J_{t+n}. So the quantum circuit for quantum phase estimation is irreducible.

8.1.6 Shor's algorithm

Shor's algorithm [Sho94] is renowned for its ability to factor integers in polynomial time. This algorithm holds particular significance because the best-known classical algorithm for factoring requires more than polynomial time, and RSA (Rivest–Shamir–Adleman), the widely-used cryptographic protocol, relies on the assumption that factoring large integers is computationally infeasible. The factoring problem is equivalent to order-finding problem, that is, given positive integers x and N with $x < N$ with no common factors, find the smallest positive integer r such that $x^r = 1 \mod N$. The quantum algorithm for order-finding is just the phase estimation algorithm applied to the unitary operator $U|y\rangle = |xy \mod N\rangle$. Since the quantum circuit for quantum phase estimation is irreducible in general, the quantum circuits for order-finding and consequently Shor's algorithm are also irreducible.

8.1.7 Grover's algorithm

Grover's algorithm [Gro96], also known as the quantum search algorithm, refers to a quantum algorithm for unstructured search that finds with high probability the unique input to a black box function that produces a particular output value, using just $O(\sqrt{N})$ evaluations of the function, where N is the size of the function's domain. Grover's algorithm consists of three main algorithms steps as illustrated in Figure 17: state preparation, the oracle U_f, and the diffusion operator U_s. The first step, state preparation, involves creating the search space, encompassing all possible cases where the solution might exist. The oracle serves the crucial role of marking the correct answers we seek within the search space. It identifies the desired solutions, making them distinguishable for measurement in the final steps of the algorithm. The oracle and diffusion operator are iteratively applied in the quantum circuit, amplifying the presence of the marked solutions until they stand out for measurement.

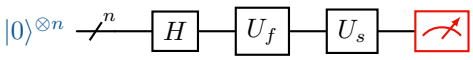

Figure 17: The Grover's algorithm.

In particular, the diffusion operator can be implemented by a multi-level controlled-CNOT gate wrapped by single-qubit gates on both sides. An illustration of the diffusion operator with $n = 4$ qubits is given below. Since the quantum circuit involves an n-qubit gate, it is clearly irreducible by Proposition 8.

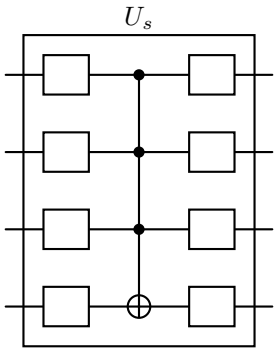

Figure 18: A quantum circuit implementation of the diffusion operator for 4-qubit Grover's algorithm. Each empty box represents a single-qubit gate.

8.1.8 Quantum counting algorithm

Quantum counting algorithm [BHT98] is a quantum algorithm designed to efficiently determine the number of solutions to a given search problem. While Grover's algorithm focuses on finding a specific solution within the oracle, the Quantum counting algorithm provides us with the ability to count how many solutions are present. The quantum circuit underlying the quantum counting algorithm essentially performs quantum phase estimation on the Grover iterator $U_s U_f$. As discussed in Section 8.1.5, the quantum circuit for quantum counting is inherently irreducible due to the irreducibility of quantum phase estimation.

8.2 Ansatzs in quantum machine learning

8.2.1 Frequently used entanglement structures

Parameterized Quantum Circuits (PQCs) serve as foundational components in quantum machine learning. These circuits usually consist of alternating rotation and entanglement layers. In the rotation layers, single-qubit rotation gates are applied to all qubits. Subsequently, the entanglement layers employ a predefined strategy to create entanglement among the qubits using double-qubit

gates. Each of these layers can be repeated multiple times to achieve the desired level of entanglement. Several commonly used entanglement layers include the following [SJAG19]:

- A linearly entangled layer of n qubits means that each qubit i is entangled with the subsequent qubit $i+1$ for $i \in \{0, 1, \cdots, n-2\}$. An example with 4 qubits is given in Figure 19a;
- A circularly entangled layer of n qubits is a linearly entangled layer with an additional entangling gate between qubit $n-1$ and qubit 0. An example with 4 qubits is given in Figure 19b;
- A pairwisely entangled layer of n qubits consists of two sub-layers. In the first sub-layer, qubit i is entangled with qubit $i+1$ for all even values of i, and in the second sub-layer, qubit i is entangled with qubit $i+1$ for all odd values of i. An example with 4 qubits is illustrated in Figure 19c;
- A fully entangled layer of n qubits means that each qubit i for $i \in \{0, 1, \cdots, n-1\}$ is entangled with qubit j for $j \in \{i, i+1, ..., n-1\}$. An example with 4 qubits is illustrated in Figure 19d.

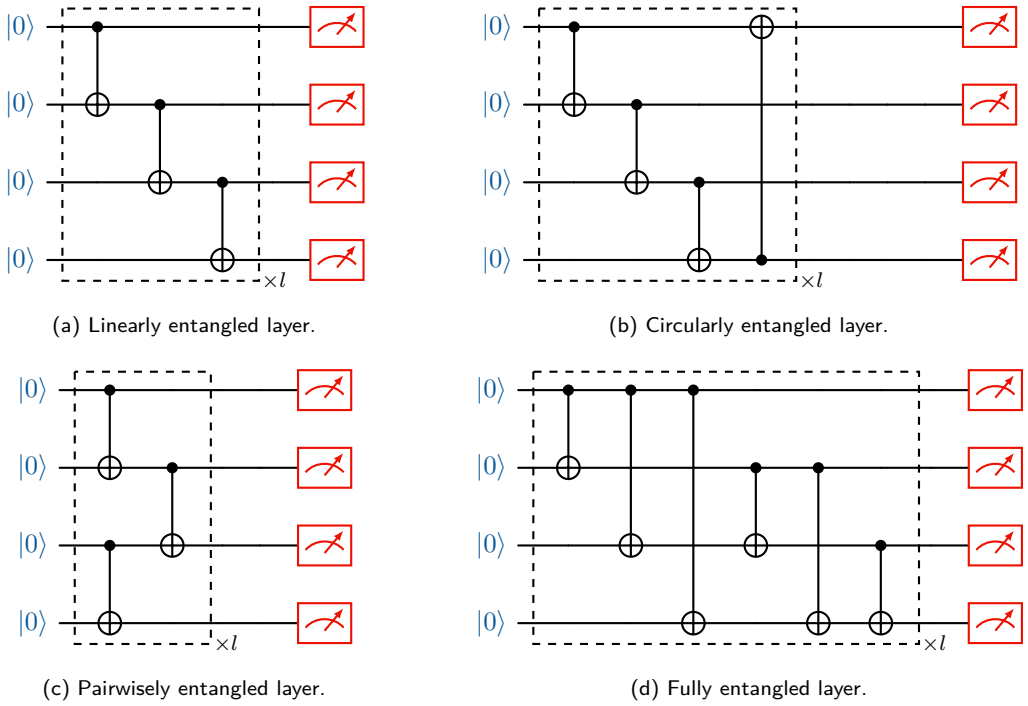

(a) Linearly entangled layer.

(b) Circularly entangled layer.

(c) Pairwisely entangled layer.

(d) Fully entangled layer.

Figure 19: Examples of four entanglement structures widely used in quantum machine learning. All single-qubit gates are omitted. Each layer in the dashed box can repeat l times.

Utilizing Proposition 8 and Theorem 11, we present the analysis of the reducibility and the optimal compilation for quantum circuits employing the four entanglement structures.

Proposition 18 (Linearly entangled quantum circuit.) *A linearly entangled quantum circuit with $n \geq 2$ qubits and $l \geq 1$ linear layers is reducible if and only if $l \leq n-2$. The corresponding optimal solution for optimization (9) can be taken at $\sum_{i=0}^{n-l-2} E^n_{i,i+l+1}$. Consequently, the circuit can be compiled to an equivalent dynamic circuit with $l+1$ qubits.*

Proof For a linearly entangled quantum circuit with layer $l = 1$, the biadjacency matrix of the simplified DAG is given by

$$B = \sum_{i=0}^{n-1} \sum_{j=\max(i-1,0)}^{n-1} E^n_{i,j}. \tag{27}$$

For any integer $l \geq 1$, we can easily check that

$$B^{\odot l} = \sum_{i=0}^{n-1} \sum_{j=\max(i-l,0)}^{n-1} E_{i,j}^{n}. \tag{28}$$

Therefore, $B^{\odot l}$ is an all-one matrix if and only if $l \geq n-1$. By Proposition 8, the biadjacency matrix for the multi-layer quantum circuit is exactly given by $B^{\odot l}$. So the circuit is irreducible if and only if $l \geq n-1$, or equivalently, it is reducible if and only if $l \leq n-2$.

Moreover, we can compute the candidate matrix for the circuit with l layers as

$$C = \sum_{i=0}^{n-l-2} \sum_{j=i+l+1}^{n-1} E_{i,j}^{n}. \tag{29}$$

For the optimal compilation, we need to select the maximum number of 1 elements in such a matrix under the conditions stated in Proposition 11. Without the nilpotent condition, the maximum number of 1 elements that simultaneously satisfies conditions (9b), (9c) and (9d) is $n-l-1$. Let us choose

$$F = \sum_{i=0}^{n-l-2} E_{i,i+l+1}^{n}, \tag{30}$$

with the total sum of $n-l-1$. Then we can easily check that the adjacency matrix with such a selection is indeed nilpotent, making it an optimal solution in (9). Finally, by Algorithm 2, the compiled circuit has circuit width $l+1$. ■

Proposition 19 (Circularly entangled quantum circuit.) *A circularly entangled quantum circuit with $n \geq 2$ qubits and $l \geq 1$ circular layers is reducible if and only if $n \geq 4$ and $l = 1$. The corresponding optimal solution for optimization (9) can be taken at $\sum_{i=1}^{n-3} E_{i,i+2}^{n}$. Consequently, the circuit can be compiled to an equivalent dynamic circuit with 3 qubits.*

Proof The proof is similar to the proof of Proposition 18. For a circularly entangled quantum circuit with layer $l = 1$, the biadjacency matrix of the simplified DAG is given by

$$B = \sum_{i=0}^{n-1} \sum_{j=\max(i-2,0)}^{n-1} E_{i,(j+1 \pmod n)}^{n}. \tag{31}$$

which is an all-one matrix if $n \leq 3$. Moreover, for any $n \geq 4$ we can check that $B^{\odot 2}$ becomes an all-one matrix. So the circuit is reducible if and only if $n \geq 4$ and $l = 1$.

Moreover, we can compute the candidate matrix for the circuit with $l = 1$ layer as

$$C = \sum_{i=1}^{n-3} \sum_{j=i+2}^{n-1} E_{i,j}^{n}. \tag{32}$$

For the optimal compilation, we need to select the maximum number of 1 elements in such a matrix under the conditions stated in Proposition 11. Without the nilpotent condition, the maximum number of 1 elements that simultaneously satisfies conditions (9b), (9c) and (9d) is $n-l-1$. Let us choose

$$F = \sum_{i=1}^{n-3} E_{i,i+2}^{n}. \tag{33}$$

with the total sum of $n-3$. Then we can easily check that the adjacency matrix with such a selection is indeed nilpotent, making it an optimal solution in (9). Finally, by Algorithm 2, the compiled circuit has circuit width 3. ■

Proposition 20 (Pairwisely entangled quantum circuit.) *A pairwisely entangled quantum circuit with $n \geq 2$ qubits and $l \geq 1$ pairwise layers is reducible if and only if $l \leq \lceil n/2 \rceil - 1$. In this case, a feasible solution for optimization (9) can be taken at $\sum_{i=0}^{n-(2l+2)} E^n_{i,i+2l+1}$ which is optimal when $l > (n-2)/4$. Consequently, the circuit can be compiled to an equivalent dynamic circuit with $2l+1$ qubits.*

Proof The proof is also similar to the proof of Proposition 18. For a pairwisely entangled quantum circuit with layer $l = 1$, the biadjacency matrix of the simplified DAG is given by

$$B = \sum_{\substack{i,j=0 \\ |i-j|\leq 1}}^{n-1} E^n_{i,j} + \sum_{\substack{i=0 \\ i \text{ even}}}^{n-3} E^n_{i,i+2} + \sum_{\substack{i=0 \\ i \text{ odd}}}^{n-3} E^n_{i+2,i} \tag{34}$$

For any integer $l \geq 1$, we can check that

$$B^{\odot l} = \sum_{\substack{i,j=0 \\ |i-j|\leq 2l-1}}^{n-1} E^n_{i,j} + \sum_{\substack{i=0 \\ i \text{ even}}}^{n-(2l+1)} E^n_{i,i+2l} + \sum_{\substack{i=0 \\ i \text{ odd}}}^{n-(2l+1)} E^n_{i+2l,i}. \tag{35}$$

Therefore, $B^{\odot l}$ is an all-one matrix if and only if $l \geq \lceil n/2 \rceil$. By Proposition 8, the biadjacency matrix for the multi-layer quantum circuit is exactly given by $B^{\odot l}$. So the circuit is irreducible if and only if $l \geq \lceil n/2 \rceil$, or equivalently, it is reducible if and only if $l \leq \lceil n/2 \rceil - 1$.

Moreover, we can compute the candidate matrix for the circuit with l layers as $C = C_L + C_R$ where

$$C_L = \sum_{\substack{i,j=0 \\ i-j\geq 2l+1}}^{n-1} E^n_{i,j} + \sum_{\substack{i=0 \\ i \text{ odd}}}^{n-(2l+1)} E^n_{i+2l,i} \tag{36}$$

$$C_R = \sum_{\substack{i,j=0 \\ j-i\geq 2l+1}}^{n-1} E^n_{i,j} + \sum_{\substack{i=0 \\ i \text{ even}}}^{n-(2l+1)} E^n_{i,i+2l} \tag{37}$$

Note that C_L and C_R have non-zero values only at the lower-left and upper-right corners of the matrix C. If $l > (n-2)/4$, the row and column indices of the non-zero entries of C_L and C_R have no intersection. So any candidate edge in C_R will contradict to any candidate edge in C_L because of the acyclic condition. If the optimal solution takes any value in C_R (or C_L), then all candidate edges are taken from C_R (or C_L).

For the optimal compilation, we need to select the maximum number of 1 elements in such a matrix under the conditions stated in Proposition 11. Without the nilpotent condition, the maximum number of 1 elements that simultaneously satisfies conditions (9b), (9c) and (9d) is $n - (2l+1)$. Let us choose

$$F = \sum_{i=0}^{n-(2l+2)} E^n_{i,i+2l+1}. \tag{38}$$

with the total sum of $n - (2l+1)$. Then we can easily check that the adjacency matrix with such a selection is indeed nilpotent, making it an optimal solution in (9). Finally, by Algorithm 2, the compiled circuit has circuit width $2l+1$. Note that when $l \leq (n-2)/4$, the above choice of F is also a feasible solution. This completes the proof. ■

Proposition 21 (Fully entangled quantum circuit.) *A fully entangled quantum circuit with $n \geq 2$ qubits and $l \geq 1$ full layers is always irreducible.*

Proof It is clear that for fully entangled quantum circuit, its biadjacencdiamond-structuredy matrix of the simplified DAG is always an all-one matrix. Therefore, the circuit is irreducible. Alternatively, the irreducibility can be easily seen from Proposition 6. ■

8.2.2 Diamond-structured quantum circuits

The Hartree-Fock method is a widely used approach in quantum chemistry for determining the electronic structure and energy of molecules and atoms. In [QC20] the authors performed a VQE simulation of the binding energy of H_6, H_8, H_{10}, H_{12} hydrogen chains where they used a variational ansatz based on basis rotations to prepare the Hartree-Fock state. Figure 20 illustrates an example of the diamond-structured basis rotation circuit used for the H_6 chain.

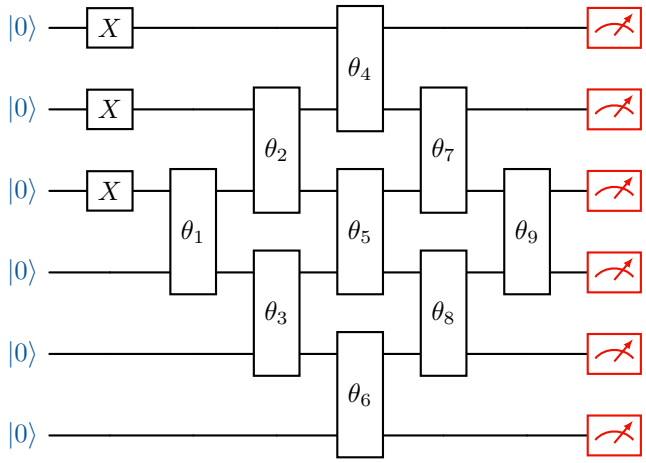

Figure 20: The diamond-structured quantum circuit for the H_6 chain. Each box with a rotation angle θ represents a double qubit rotation gate.

The subsequent proposition provides the optimal compilation of the diamond-structured circuit designed to prepare the Hartree-Fock state.

Proposition 22 (Diamond-structured quantum circuit) *A diamond-structured circuit for linear chain of $2n$ hydrogen atoms with $2n$ qubits is always reducible. The corresponding optimal solution for optimization (9) can be taken at $\sum_{i=0}^{n-2} E^{2n}_{i,i+n+1}$. Consequently, the circuit can be compiled to an equivalent dynamic circuit with $n+1$ qubits.*

Proof For a diamond-structured circuit with $2n$ qubits, the biadjacency matrix of the simplified DAG is given by

$$B = \sum_{i=0}^{n-1} \sum_{j=0}^{i+n} E^{2n}_{i,j} + \sum_{i=n}^{2n-1} \sum_{j=i-n}^{2n-1} E^{2n}_{i,j} \tag{39}$$

We can further compute the candidate matrix for the circuit as $C = C_L + C_R$ where

$$C_L = \sum_{i=n+1}^{2n-1} \sum_{j=0}^{i-n-1} E^{2n}_{i,j} \tag{40}$$

$$C_R = \sum_{i=0}^{n-2} \sum_{j=i+n+1}^{2n-1} E^{2n}_{i,j} \tag{41}$$

It is worth noting that the matrices C_L and C_R contain non-zero entries only at the lower-left and upper-right corners. Since there is no overlap in the row and column indices of the non-zero entries between C_L and C_R, any candidate edge in C_L would conflict with any candidate edge in C_R because of the acyclic condition. Consequently, if the optimal solution selects any edge from C_R (or C_L), it necessitates that all candidate edges are drawn exclusively from C_R (or C_L).

To achieve the optimal compilation, our objective is to maximize the number 1 elements in such a matrix under the conditions stated in Proposition 11. In the absence of the nilpotent condition,

we have the flexibility to select

$$F = \sum_{i=0}^{n-2} E_{i,i+n+1}^{2n} \tag{42}$$

with the total sum of $n-1$. Then we can easily check that the adjacency matrix with such a selection is indeed nilpotent, making it an optimal solution in (9). Finally, by Algorithm 2, the compiled circuit has circuit width $n+1$, which completes the proof. ■

8.3 Measurement-based quantum computation

Measurement-based quantum computation (MBQC) constitutes an alternative quantum computation model. This model guides the computation process by measuring a portion of the qubits within an entangled state, while the remaining unmeasured qubits evolve correspondingly. The MBQC computation can be divided into three primary steps. The initial step involves preparing a resource state, which is a highly entangled many-body quantum state. This state can be pre-generated offline and is independent of specific computational tasks. Subsequently, the second step entails sequentially performing single-qubit measurements on each qubit of the prepared resource state. These measurements might be adaptive, meaning that later measurement choices can depend on the outcomes of prior measurements. In the third step, classical data processing is applied to the measurement outcomes in order to derive the necessary computational results. An illustration of the resource state is provided in Figure 21(a), where the grid signifies a widely used quantum resource state referred to as the cluster state. Within this grid, each vertex represents a qubit (typically initialized as a plus state $|+\rangle = (|0\rangle + |1\rangle)/\sqrt{2}$), while edges connecting the vertices symbolize controlled-phase gates operating on the linked qubits.

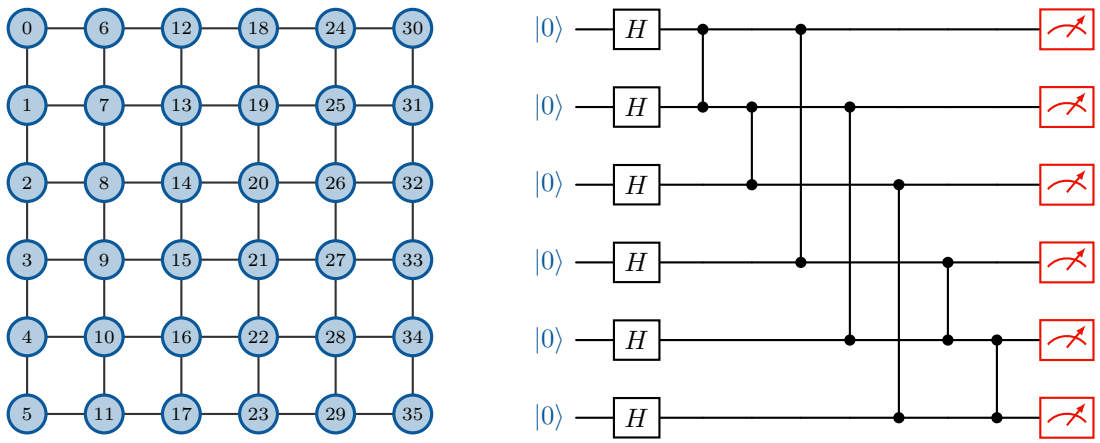

(a) Cluster state of size $(6, 6)$.

(b) Cluster-state quantum circuit of size $(3, 2)$.

Figure 21: An example of cluster state and cluster-state quantum circuit.

Measurement-based quantum computation plays a pivotal role in blind quantum computation, a cloud-based quantum computing scheme that enables users to conduct calculations privately in a quantum network without disclosing any information to the server [Fit17]. This capability holds great promise for the future quantum internet. Nonetheless, the standard approach of quantum computation in cloud servers typically operates in the quantum circuit model. Integrating an MBQC algorithm into this model necessitates a considerable number of qubits. Specifically, MBQC applied to a cluster state of size (w, d)—where w signifies the number of rows and d signifies the number of columns—can be translated directly into a quantum circuit of size wd. We refer to this circuit as a *cluster-state quantum circuit* of size (w, d). As shown in Figure 21(b), an initial Hadamard gate is applied to each qubit to prepare a plus state. Subsequently, controlled-phase gates are employed based on the topology of the grid. Finally, a measurement is taken on each

qubit. It is important to note that measurements are typically applied sequentially to the qubits column by column. Measurements on the same column are independent, while measurements on later columns may depend on the results of the previous columns.

The reducibility of cluster-state quantum circuits depends on the order of the controlled-phase gates. The following result is based on the specific order in which we implement the controlled-phase gates. First, we implement the gates in the first column, then those between the first and second columns, and so on. Additionally, the qubits in the first column of a cluster state can be initialized in an entangled quantum state.

The following result demonstrates that this circuit can be effectively reduced to a dynamic quantum circuit with $w+1$ qubits, which is independent of the parameter d. This reduction significantly reduces the resource requirements for running MBQC algorithms on quantum computers that are primarily designed for circuit-based operations.

Proposition 23 (Cluster-state quantum circuit.) *A cluster-state quantum circuit of size (w, d) is reducible for any $d \geq 2$. The corresponding optimal solution for optimization (9) can be taken at $\sum_{i=0}^{wd-(w+2)} E^{wd}_{i,i+w+1}$ in general. Consequently, the circuit can be compiled to an equivalent dynamic circuit with $w+1$ qubits.*

Proof For a cluster-state quantum circuit of size (w, d), its biadjacency matrix of the simplified DAG is given by a block matrix:

$$B = \sum_{i=1}^{d-1} E^{d}_{i,i-1} \otimes I_w + \sum_{i=0}^{d-1} \sum_{j=0}^{d-i-1} E^{d}_{i,i+j} \otimes D_j \tag{43}$$

where each block

$$D_k = \sum_{i=0}^{w-1} \sum_{j=\max(i-k-1,0)}^{w-1} E^{w}_{i,j}. \tag{44}$$

We can further compute the candidate matrix as

$$C = \sum_{i=0}^{d-1} \sum_{j=0}^{i} E^{d}_{i,i-j} \otimes G_j + \sum_{i=0}^{d-2} E^{d}_{i,i+1} \otimes (J_w - I_w) + \sum_{i=0}^{d-1} \sum_{j=i+2}^{d-1} E^{d}_{i,j} \otimes J_w, \tag{45}$$

where

$$G_k = \sum_{i=0}^{w-1} \sum_{j=i+k+2}^{w-1} E^{w}_{i,j}. \tag{46}$$

We need to select as many as 1 elements within the conditions stated in Proposition 11. Without the nilpotent condition, we can choose

$$F = \sum_{i=0}^{wd-(w+2)} E^{wd}_{i,i+w+1}. \tag{47}$$

which simultaneously satisfies conditions (9b), (9c) and (9d). Then we can easily check that the adjacency matrix with such a selection is indeed nilpotent, making it a feasible solution in (9). Finally, by Algorithm 2, the compiled circuit has circuit width $w+1$. Since the quantum state in the first column of qubits can be assigned to an arbitrary global quantum state in general, this requires at least w qubits. Moreover, no matter which qubit in the first column to measure first, we need at least one more qubit to apply for the controlled-phase gate between the qubit to measure and the adjacent qubit on its right. This makes the circuit has at least $w+1$ qubits, indicating the optimality of our compilation. ■

Remark 9 Similar compilations also work for measurement-based quantum computation with other graph states, such as the brickwork state used in [BFK09].

8.4 Quantum supremacy circuits

To compare the reducibility of quantum circuits as well as the performance of different compilation methods, we define the *reducibility factor* of a quantum circuit as

$$r = 1 - \frac{n'}{n} \in [0, 1), \tag{48}$$

where n is the width of the original circuit and n' is the width of the compiled circuit. This factor characterizes the extent to which the circuit width can be reduced by a certain algorithm, which is zero if the circuit is not reducible.

In this section, we analyze the reducibility factor of quantum circuits used to claim quantum supremacy, including those executed on Sycamore and Zuchongzhi quantum computers. Figure 22 displays the reducibility factor of quantum supremacy circuits with varying numbers of cycles, determined using the greedy heuristic algorithm (Algorithm 7).

An interesting observation emerges from this analysis. Quantum circuits with 70 qubits and 24 cycles running on Sycamore [MVM+23], 56 qubits and 20 cycles on Zuchongzhi [WBC+21], and 60 qubits and 24 cycles on Zuchongzhi [ZCC+22] are all irreducible circuits. This observation underscores the inherent trade-off between the technical challenges associated with running deep circuits (a limitation of current quantum computers) and the structural complexity of these circuits (a limitation of classical computers). It highlights the delicate balance required when designing quantum circuits to showcase quantum supremacy in the near term.

Furthermore, another noteworthy point is the quantum circuit with 53 qubits and 20 cycles executed on Sycamore [AAB+19], which possesses a reducibility factor of 0.02. This result indicates that the circuit can be compiled into a quantum circuit with 52 qubits. This observation aligns with the historical fact that one qubit on the Sycamore chip is non-functional, thereby breaking the complexity of the circuit and leaving the room for its compilation.

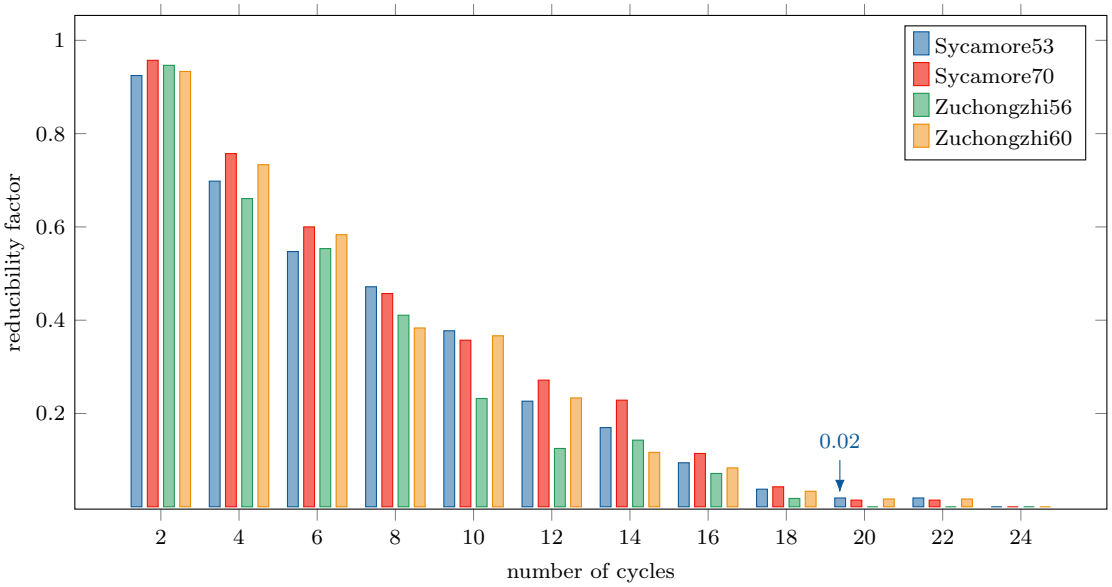

Figure 22: The reducibility factor of different quantum supremacy circuits using the greedy heuristic algorithm 7.

In 2018, Google proposed a series of random quantum circuits (GRCS[2]) [BIS+18]. Due to the hardness of simulation, GRCS is frequently used as benchmark to test the performance of classical simulators. Each instance in GRCS is a random quantum circuit designed for qubits configured in an $n \times m$ lattice. These circuits are composed of multiple cycles of quantum gates. The initial cycle is a layer of Hadamard gates acting on all qubits. Subsequent cycles exhibit a structured arrangement, starting with a layer of controlled-phase (CZ) gates placed alternatively according to some pre-defined patterns, followed by a layer of single-qubit gates randomly selected from the set

[2] https://github.com/sboixo/GRCS

$\{X^{1/2}, Y^{1/2}, T\}$. Notably, these single-qubit gates are applied exclusively to qubits not occupied by the CZ gates within the same cycle. The following Figure 23 shows the reducibility factor of GRCS circuits by running the greedy heuristic algorithm 7 once. It can be seen that the larger the number of cycles (depth), the more difficult for a quantum circuit to reduce.

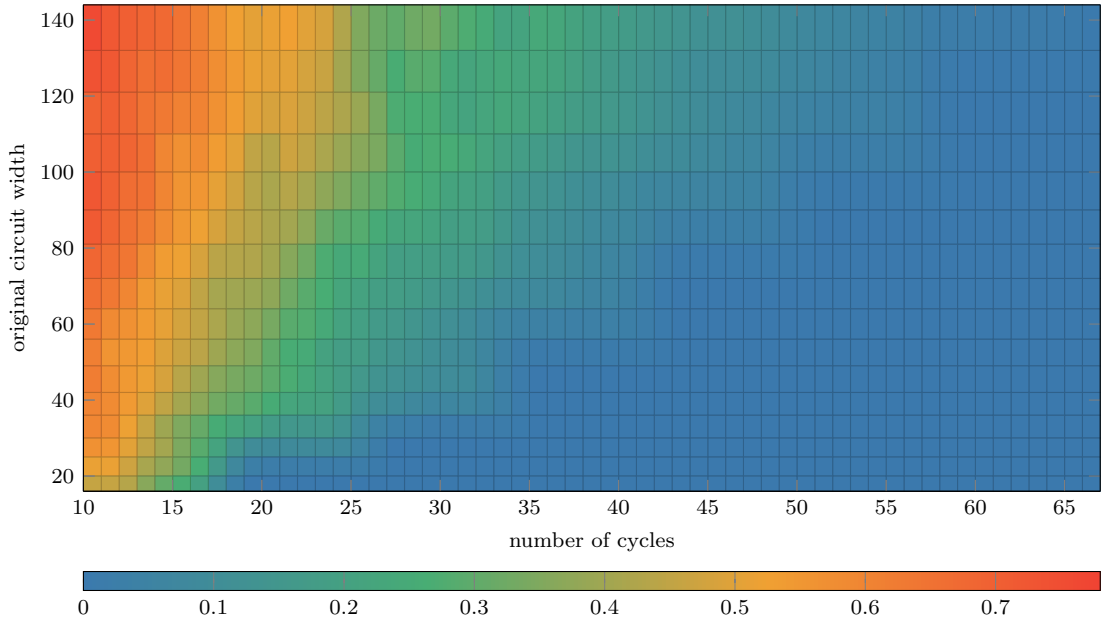

Figure 23: The reducibility factor of GRCS circuits located in the GitHub directory 'inst/rectangular' with different circuit widths and numbers of cycles using the greedy heuristic algorithm 7.

8.5 Algorithm benchmarking

In this section, we conduct a numerical analysis to assess the performance of different algorithms on a range of benchmark circuits, including quantum adders, GRCS circuits, quantum approximate optimization algorithm (QAOA), and random quantum circuits. Our primary focus centers around three distinct algorithms for dynamic circuit compilation: the MRV heuristic algorithm (Algorithm 6), the greedy heuristic algorithm (Algorithm 7) and the greedy algorithm proposed in [DCKFF22] (referred to as DCKF in the subsequent discussion). As the source code for the DCKF algorithm is not publicly available, we have implemented the DCKF algorithm based on our understanding of the paper [DCKFF22]. Further details regarding our implementation of the DCKF algorithm can be found in Appendix B. For the MRV algorithm, we perform two separate runs, swapping the roles of roots and terminals within the algorithm for each run. Subsequently, we select the dynamic circuit with the smaller circuit width as the final output. We have also implemented our greedy heuristic algorithm multiple times to improve its performance.

8.5.1 Quantum Ripple Carry Adders

Quantum adder is a quantum circuit designed for performing addition operation between two bit strings. For example, if we compute '$1 + 2 = 3$', then we represent the input string as '01' and '10', and the expected output bit string is '11'. Here we focus on the Quantum Ripple Carry Adders initially proposed in [CSK08]. These circuits are composed of $3k + 1$ qubits where the additional qubit is used to store the carry bit and rely on CNOT and Toffoli gates as foundational components. The implementation of a 2-bit quantum adder circuit is illustrated in Figure 24.

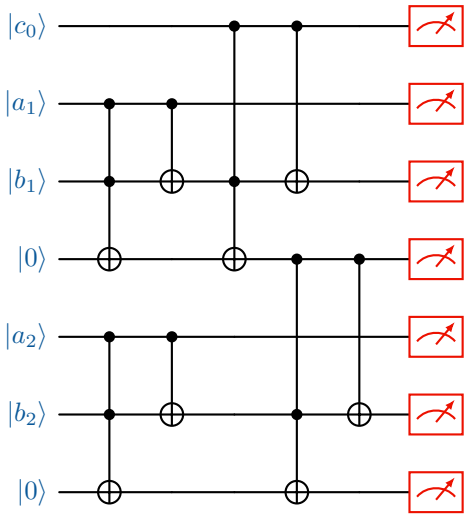

Figure 24: The implementation of a 2-bit quantum ripple carry adder circuit to calculate $a_2a_1 + b_2b_1$.

The optimal compilation of quantum ripple carry adder with $n = 3k + 1$ qubits is given in the following proposition.

Proposition 24 (Quantum ripple carry adder.) *A quantum ripple carry adder circuit with n qubits is always reducible. The corresponding optimal solution for optimization (9) can be taken at $\sum_{i=0}^{n-5} E^n_{i,i+4}$ for general cases and $E_{1,0}$ for $n = 4$. Consequently, the circuit can be compiled to an equivalent dynamic circuit with 4 qubits for $n \geq 5$ and 3 qubits for $n = 4$.*

Proof For a quantum ripple carry adder circuit with 4 qubits, the candidate matrix only has one non-zero entry, therefore the optimal compilation gives 3 qubits. For a quantum adder circuit with $n = 3k + 1 > 4$ qubits, the biadjacency matrix of the simplified DAG is given by

$$B = \sum_{i=0}^{3}\sum_{j=0}^{n-1} E^n_{i,j} + \sum_{m=1}^{k-1}\sum_{i=3m+1}^{3m+3}\sum_{j=3m}^{n-1} E^n_{i,j} - \sum_{j=0}^{k-1}\sum_{i=0}^{3j} E^n_{i,3j+1}. \tag{49}$$

The candidate matrix can be further computed as

$$C = \sum_{i=1}^{k}\sum_{j=0}^{n-3i-1} E^n_{n-3i,j} + \sum_{m=0}^{k-2}\sum_{i=3m}^{3m+2}\sum_{j=3m+4}^{n-1} E^n_{i,j}. \tag{50}$$

We need to select as many as 1 elements within the conditions stated in Proposition 11. Without taking into account the nilpotent condition, we can choose

$$F = \sum_{i=0}^{n-5} E^n_{i,i+4} + E_{n-3,l} \tag{51}$$

where $l \in [0, n-4]$. However, upon closer examination, it becomes evident that each of these candidate edges $E_{n-3,l}$ conflicts with the edge $E_{n-5,n-1}$ due to the nilpotent condition. Therefore, our selection is constrained to

$$F = \sum_{i=0}^{n-5} E^n_{i,i+4} \tag{52}$$

we can easily verify that the adjacency matrix with such a selection is indeed nilpotent, making it the optimal solution in (9). Finally, by Algorithm 2, the compiled circuit has circuit width 4. This can be easily understood as the quantum ripple carry adder employs Toffoli gates, therefore

requiring a minimum of three qubits, while an additional qubit serving as a carry-over between distinct adders. ■

In Figure 25, we present the results of the numerical experiments conducted using three different algorithms. It is evident that both MRV and the greedy algorithm successfully find the optimal compilation. In contrast, the results obtained from the DCKF algorithm show a linear scaling in the original circuit width, indicating a deficiency in its performance. This limitation can be attributed to a specific aspect of its implementation. To elaborate, when determining the measurement order in the DCKF algorithm, certain scenarios lead to the emergence of multiple local optima within a single iteration. In such cases, a deterministic selection may result in an unfavorable measurement order, ultimately impacting the overall performance. This challenge underscores the reasoning behind our inclusion of randomness within our greedy heuristic algorithm (Algorithm 7).

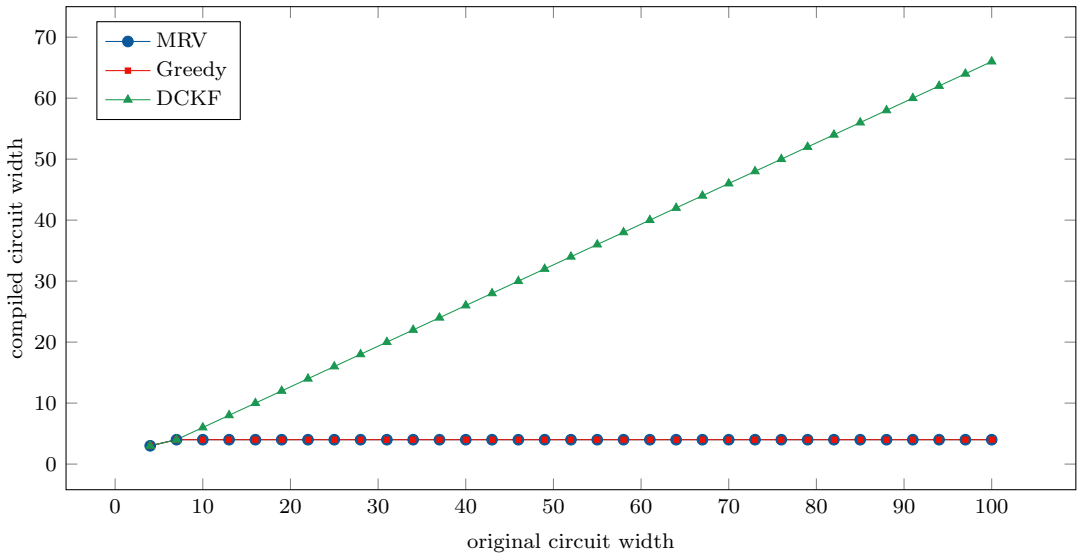

Figure 25: Compiled circuit width against the original circuit width of quantum ripple carry adders.

8.5.2 GRCS circuits

We also benchmark the three algorithms on GRCS circuits with 13 cycles. During this experiment, we ran the greedy heuristic algorithm 10 times and recorded the best result. The results in Figure 26 indicate that our greedy heuristic algorithm outperforms the DCKF algorithm in most cases.

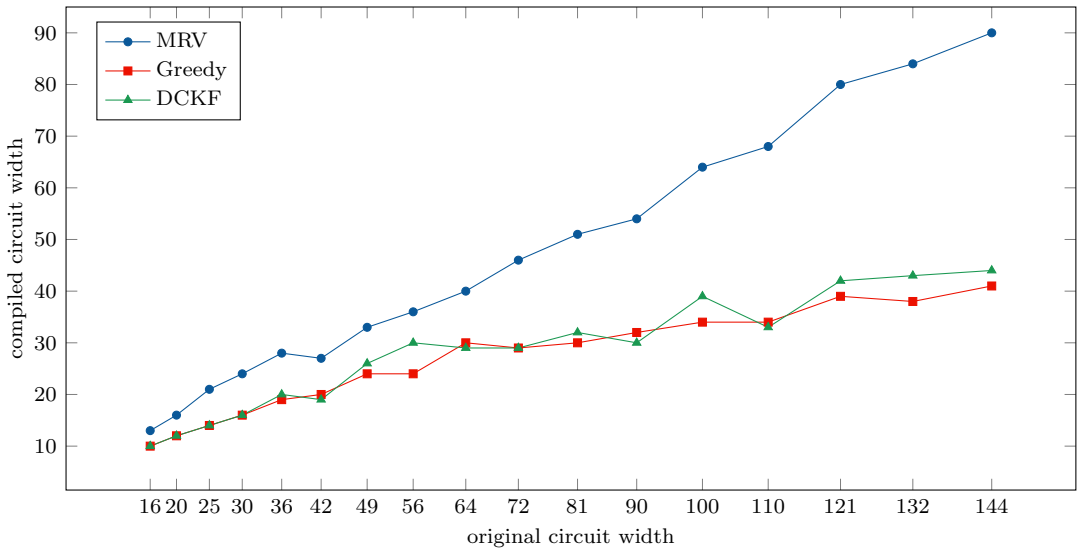

Figure 26: Compiled circuit width against the original circuit width of GRCS circuits with 13 cycles.

8.5.3 QAOA circuits for max-cut problem

Quantum approximate optimization algorithm (QAOA) [FGG14] is a quantum algorithm designed to approximately solve classical combinatorial optimization problems and have the potential to run on near-term quantum devices. The QAOA unitary is composed of the alternative application of a mixing unitary $U_B(\beta_i) = e^{-i\beta_i H_B}$ and a problem unitary $U_C(\gamma_i) = e^{-i\gamma_i H_C}$ for p layers:

$$U(\vec{\gamma}, \vec{\beta}) = \prod_{i=1}^{p} U_B(\beta_i) U_C(\gamma_i) \tag{53}$$

where H_B is the mixing Hamiltonian and H_C is the problem Hamiltonian.

A max-cut problem is a combinatorial optimization problem in graph theory which involves to find a partition of vertices into two sets, such that the number of edges between the sets is maximized. The mixing Hamiltonian and the problem Hamiltonian in a max-cut problem on an unweighted graph $G(V, E)$ takes the form of:

$$H_B = \sum_{i \in V} X_i, \tag{54}$$

$$H_C = \frac{1}{2} \sum_{(j,k) \in E} (1 - Z_j Z_k). \tag{55}$$

It is evident that in QAOA circuits designed for solving the max-cut problem, the number of qubits matches the number of vertices in the graph, and the connectivity of double-qubit gates corresponds to the edges in the graph. Here, we assess the performance of different algorithms applied to QAOA circuits for solving the max-cut problem on random unweighted three-regular (U3R) graphs with $p = 1$. For each experiment, we ran our greedy heuristic algorithm 10 times and recorded the best result. We evaluated three algorithms for each fixed qubit number on 20 random U3R graphs generated using the *NetworkX* package [HSS08]. The results are presented in Figure 27. It is evident that the average compiled width achieved by our greedy algorithm is consistently lower than that obtained using the DCKF algorithm for all qubit numbers. Moreover, as the number of qubits increases, this advantage becomes increasingly pronounced.

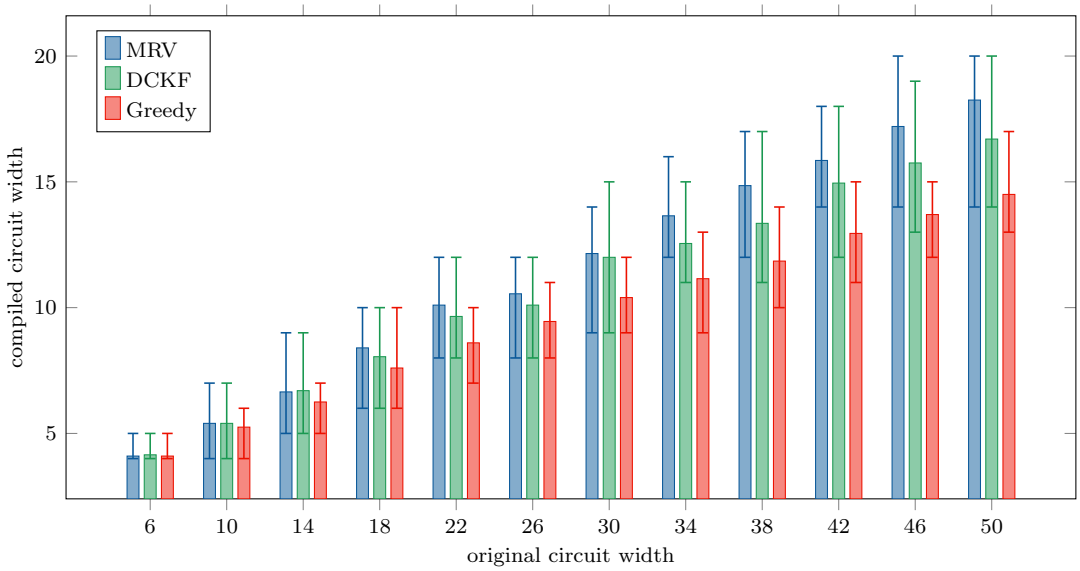

Figure 27: Compiled circuit width against the original circuit width of the max-cut QAOA circuits with $p = 1$. The plotted error bars correspond to the maximum and minimum compiled width over 20 evaluated instances.

8.5.4 Random circuits

In addition to the previously studied structured circuit examples, we conducted comprehensive numerical experiments involving random quantum circuits to assess algorithm performance across

a broader spectrum of scenarios. These experiments involved fixing the ratio $r = m/n$, where m represents the number of double-qubit gates, and n represents the width of the original circuits. We uniformly and randomly selected a qubit number from the range between 10 and 80 and sampled the desired number of double-qubit gates to construct the circuit.

We evaluated the reducibility factor using both our greedy heuristic and the DCKF algorithm on these randomly generated circuits. For each fixed ratio, we sampled 300 random circuits and ran our greedy algorithm 15 times for each circuit. The results, presented in Figure 28, demonstrate that our greedy heuristic (vertical) outperforms the DCKF algorithm (horizontal) in approximately 87.6% of cases, with a strict advantage over 49.6% of random circuits. Furthermore, as illustrated in the zoomed-in figure, our advantage is particularly pronounced when the reducibility factors are large (corresponding to a small ratio r), with our algorithm outperforming in approximately 98.5% of such instances.

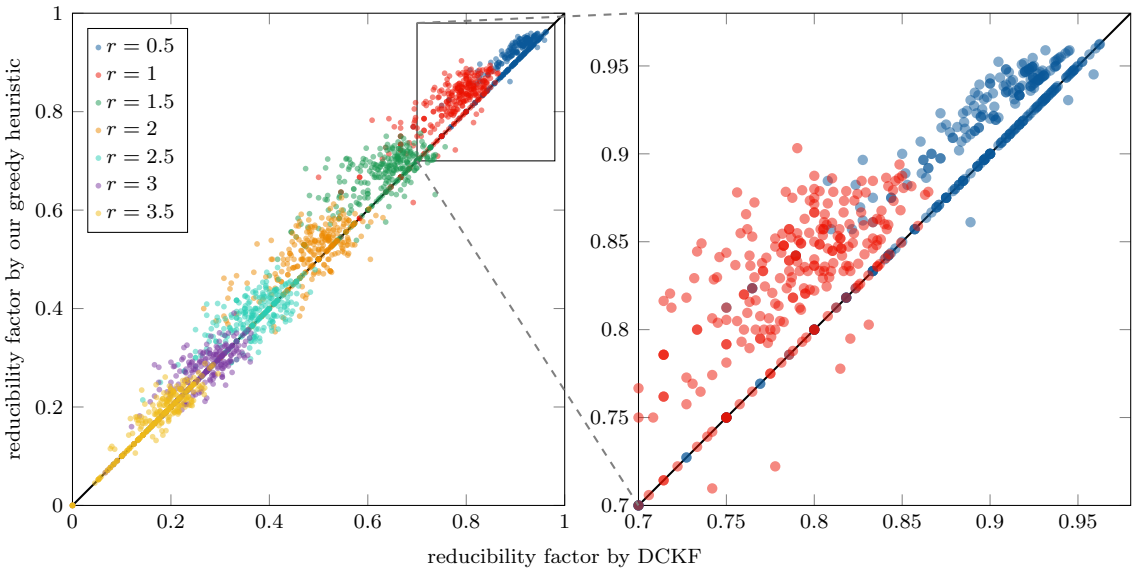

Figure 28: The reducibility factor of the randomly generated quantum circuits evaluted using our greedy heuristic algorithm 7 and the DCKF algorithm. The figure on the right provides a closer look at the region where the reducibility factors are relatively large. The black reference line indicates when the reducibility factors are equal for both algorithms.

8.5.5 Hierarchy Levels in Hybrid Algorithm

To demonstrate the trade-off between solution optimality and computational time complexity, we assessed the performance and runtime of the hybrid algorithm (Algorithm 8) at various hierarchy levels (0, 1, 2, 3) for max-cut QAOA circuits on U3R graphs with $p = 1$. The numerical experiments were conducted on a MacBook Pro (2020) with an Intel i5 processor and 16GB memory. Figure 29 depicts the average compiled circuit width and algorithm runtime over 20 random graphs for each qubit number. As expected, the results show that as the hierarchy level increases, we attain better compilations. However, the algorithm runtime also increases proportionally. Therefore, the hybrid algorithm shall be a suitable choice for scenarios where minimizing the compiled circuit width is of top priority, provided that the runtime remains within acceptable limits.

9 Discussion

In this work, we conducted a comprehensive investigation into the dynamic circuit compilation, aiming to convert static quantum circuits into equivalent dynamic circuits with fewer qubits through qubit-reuse. We initiated our exploration by introducing the first characterization of this task through graph manipulation and developed a precise mathematical model for optimal compilation. Within this framework, we introduced efficient algorithms to determine the reducibility of a static quantum circuit from various perspectives and presented several heuristic algorithms with

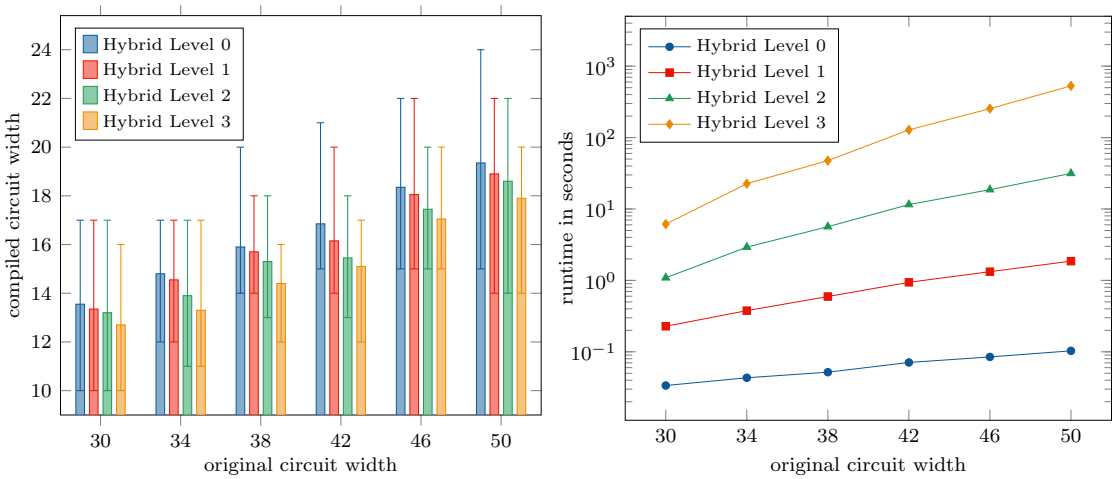

Figure 29: Compiled circuit width (left) and algorithm runtime in seconds (right) as a function of the original circuit width of max-cut QAOA with $p = 1$, compiled by hybrid algorithm 8 with different hierarchy levels. The ploted error bars in the left figure correspond to the maximum and the minimum compiled width over 20 evaluated instances. The runtime in the right figure represents the average runtime.

the objective of minimizing the qubit requirements for the compiled circuits. The effectiveness of our approach was demonstrated through a multifaceted approach which included theoretical analyses of reducibility and optimal compilation for various renowned quantum circuits, as well as a numerical evaluation of our heuristic algorithms on a wide range of benchmark circuits. Notably, the comparative analysis with existing algorithms unveiled the superior of our method in a plethora of cases. Finally, it is worth noting that the dynamic circuit compilation explored in this work offers a complementary strategy to other circuit optimization techniques and can be seamlessly integrated with existing methods. For example, it can be applied after the removal of redundant gates or before mapping the circuit to a specific quantum hardware architecture.

Several open problems remain for future research. The most significant one pertains to extending the approach outlined in this paper to dynamic quantum circuits. Specifically, we can consider to begin with a dynamic quantum circuit and seek to compile it into a circuit with a smaller width. However, this extension introduces greater complexities, as it necessitates determining whether a given dynamic quantum circuit can be further reduced in terms of qubit count. This problem is intricately linked to the optimality of quantum circuit compilation. Therefore, it is crucial to emphasize that the applicability of our reducibility checking approaches, as proposed in Propositions 4, 6 and 9, is currently limited to static circuits. We provide an illustrative example in Appendix A to highlight the challenges and considerations involved in compiling a dynamic quantum circuit.

Furthermore, we have noted a remarkable similarity between the graph optimization problem explored in this work and the well-established Maximum Acyclic Subgraph (MAS) problem in graph theory. The MAS problem for a graph (V, E) involves identifying a subgraph (V, E') with $E' \subseteq E$, such that it contains no cycles and has the maximum number of edges. Our problem can be reformulated as a constrained version of the MAS problem. Let (V, E) be the simplified DAG and $\bar{E}$ be the set of candidate edges. We can first incorporate all candidate edges into the simplified DAG and try to identify the maximum acyclic subgraph in the resultant graph $(V, E \cup \bar{E})$ under the additional constraint that only edges in set $\bar{E}$ can be removed. Suppose the solution to this problem yields a subgraph $(V, E \cup \bar{E}')$ where $\bar{E}' \subseteq \bar{E}$, then the maximum matching in the graph $(V, \bar{E}')$ corresponds to a feasible solution to our problem. It is worth noting that the MAS problem has been well-established as a NP-hard problem [Kar72]. Therefore, we expect that the optimal compilation of a quantum circuit may similarly belong to the class of NP-hard. However, the formal proof of its NP-hardness remains open. Additionally, several algorithms have been proposed in the literature to find approximate solutions for the MAS problem [HR94, CP20], which may offer valuable insights for seeking approximate solutions to the dynamic circuit compilation.

Finally, quantum circuits serve as practical implementations of quantum algorithms, and in

many instances of interest, a quantum circuit is not unique but can be expressed using different combinations of quantum gates. An illustrative example can be found in a cluster-state quantum circuit of size $(2, 2)$. When the controlled-phase gates are implemented column by column, the resulting circuit can be reduced to just 3 qubits. However, if we implement the controlled-phase gates row by row, then the circuit becomes irreducible. This observation leads to a challenging question: Can we extend the concept of reducibility beyond the level of quantum circuits and into the realm of quantum algorithms? Alternatively, can we develop a framework capable of achieving dynamic circuit compilation independently of specific circuit implementations? This question merits further consideration and may open up a compelling avenue for research in the field of quantum circuit optimization and quantum algorithm design.

Acknowledgements

We would like to thank Jingtian Zhao for part of the code implementation in QNET. This work was done when M. Z. and R. S. were research interns at Baidu Research. Y. L. is supported by the National Nature Science Foundation of China (No. 62302346) and supported by "the Fundamental Research Funds for the Central Universities".

References

[AAB+19] Frank Arute, Kunal Arya, Ryan Babbush, Dave Bacon, Joseph C. Bardin, Rami Barends, Rupak Biswas, Sergio Boixo, Fernando G. S. L. Brandao, David A. Buell, et al. Quantum supremacy using a programmable superconducting processor. *Nature*, 574(7779):505–510, Oct 2019, 10.1038/s41586-019-1666-5.

[AG04] Scott Aaronson and Daniel Gottesman. Improved simulation of stabilizer circuits. *Physical Review A*, 70(5):052328, Nov 2004, 10.1103/PhysRevA.70.052328.

[AI23] Google Quantum AI. Suppressing quantum errors by scaling a surface code logical qubit. *Nature*, 614(7949):676–681, Feb 2023, 10.1038/s41586-022-05434-1.

[BBC+93] Charles H Bennett, Gilles Brassard, Claude Crépeau, Richard Jozsa, Asher Peres, and William K Wootters. Teleporting an unknown quantum state via dual classical and Einstein-Podolsky-Rosen channels. *Physical Review Letters*, 70(13):1895–1899, Mar 1993, 10.1103/PhysRevLett.70.1895.

[BFK09] Anne Broadbent, Joseph Fitzsimons, and Elham Kashefi. Universal blind quantum computation. In *2009 50th Annual IEEE Symposium on Foundations of Computer Science*, pages 517–526. IEEE, Oct 2009. 10.1109/focs.2009.36.

[BHT98] Gilles Brassard, Peter Høyer, and Alain Tapp. Quantum counting. In *Automata, Languages and Programming: 25th International Colloquium, ICALP'98 Aalborg, Denmark, July 13–17, 1998 Proceedings 25*, pages 820–831. Springer, 1998. 10.1007/BFb0055105.

[BIS+18] Sergio Boixo, Sergei V Isakov, Vadim N Smelyanskiy, Ryan Babbush, Nan Ding, Zhang Jiang, Michael J Bremner, John M Martinis, and Hartmut Neven. Characterizing quantum supremacy in near-term devices. *Nature Physics*, 14(6):595–600, Apr 2018, 10.1038/s41567-018-0124-x.

[BJG08] Jørgen Bang-Jensen and Gregory Z Gutin. *Digraphs: theory, algorithms and applications*. Springer Science & Business Media, 2008.

[BPK23] Sebastian Brandhofer, Ilia Polian, and Kevin Krsulich. Optimal qubit reuse for near-term quantum computers, 2023. arXiv:2308.00194.

[BSHM21] Sergey Bravyi, Ruslan Shaydulin, Shaohan Hu, and Dmitri Maslov. Clifford circuit optimization with templates and symbolic pauli gates. *Quantum*, 5:580, Nov 2021, 10.22331/q-2021-11-16-580.

[BV97] Ethan Bernstein and Umesh Vazirani. Quantum complexity theory. *SIAM Journal on Computing*, 26(5):1411–1473, Oct 1997, 10.1137/S0097539796300921.

[BWP+17] Jacob Biamonte, Peter Wittek, Nicola Pancotti, Patrick Rebentrost, Nathan Wiebe, and Seth Lloyd. Quantum machine learning. *Nature*, 549(7671):195–202, Sep 2017, 10.1038/nature23474.

[con23] Qiskit contributors. Qiskit: An open-source framework for quantum computing, 2023, 10.5281/zenodo.2573505.

[CP20] Aleksandar Cvetković and Vladimir Yu. Protasov. Maximal acyclic subgraphs and closest stable matrices. *SIAM Journal on Matrix Analysis and Applications*, 41(3):1167–1182, Aug 2020, 10.1137/19M1305422.

[CSK08] Amlan Chakrabarti and Susmita Sur-Kolay. Designing quantum adder circuits and evaluating their error performance. In *2008 International Conference on Electronic Design*, pages 1–6. IEEE, Dec 2008. 10.1109/ICED.2008.4786689.

[CTI+21] A. D. Córcoles, Maika Takita, Ken Inoue, Scott Lekuch, Zlatko K. Minev, Jerry M. Chow, and Jay M. Gambetta. Exploiting dynamic quantum circuits in a quantum algorithm with superconducting qubits. *Physical Review Letters*, 127(10):100501, Aug 2021, 10.1103/PhysRevLett.127.100501.

[DCKFF22] Matthew DeCross, Eli Chertkov, Megan Kohagen, and Michael Foss-Feig. Qubit-reuse compilation with mid-circuit measurement and reset, 2022. arXiv:2210.08039.

[Deo16] Narsingh Deo. *Graph theory with applications to engineering and computer science*. Dover Publications, 2016.

[DJ92] David Deutsch and Richard Jozsa. Rapid solution of problems by quantum computation. *Proceedings of the Royal Society of London. Series A: Mathematical and Physical Sciences*, 439(1907):553–558, Dec 1992, 10.1098/rspa.1992.0167.

[FGG14] Edward Farhi, Jeffrey Goldstone, and Sam Gutmann. A quantum approximate optimization algorithm, 2014. arXiv:1411.4028.

[Fit17] Joseph F. Fitzsimons. Private quantum computation: an introduction to blind quantum computing and related protocols. *npj Quantum Information*, 3(1):23, Jun 2017, 10.1038/s41534-017-0025-3.

[FMMC12] Austin G. Fowler, Matteo Mariantoni, John M. Martinis, and Andrew N. Cleland. Surface codes: Towards practical large-scale quantum computation. *Physical Review A*, 86(3):032324, Sep 2012, 10.1103/PhysRevA.86.032324.

[FZL+23] Kun Fang, Jingtian Zhao, Xiufan Li, Yifei Li, and Runyao Duan. Quantum NETwork: from theory to practice. *Science China Information Sciences*, 66(8):180509, Jul 2023, 10.1007/s11432-023-3773-4.

[Gro96] Lov K. Grover. A fast quantum mechanical algorithm for database search. In *Proceedings of the twenty-eighth annual ACM symposium on Theory of Computing*, pages 212–219. Association for Computing Machinery, Jul 1996. 10.1145/237814.237866.

[HJC+23] Fei Hua, Yuwei Jin, Yanhao Chen, Suhas Vittal, Kevin Krsulich, Lev S. Bishop, John Lapeyre, Ali Javadi-Abhari, and Eddy Z. Zhang. Exploiting qubit reuse through mid-circuit measurement and reset, 2023. arXiv:2211.01925.

[HR94] Refael Hassin and Shlomi Rubinstein. Approximations for the maximum acyclic subgraph problem. *Information Processing Letters*, 51(3):133–140, Aug 1994, 10.1016/0020-0190(94)00086-7.

[HSS08] Aric A. Hagberg, Daniel A. Schult, and Pieter J. Swart. Exploring network structure, dynamics, and function using NetworkX. In *Proceedings of the 7th Python in Science Conference*, pages 11 – 15. Scipy2008, Aug 2008.

[Kar72] Richard M. Karp. Reducibility among combinatorial problems. In *Complexity of Computer Computations: Proceedings of a symposium on the Complexity of Computer Computations*, pages 85–103. Plenum Press, Mar 1972. 10.1007/978-1-4684-2001-2_9.

[KG00] Navin Khaneja and Steffen Glaser. Cartan decomposition of $SU(2^n)$, constructive controllability of spin systems and universal quantum computing, 2000. arXiv:quant-ph/0010100.

[LQW+22] Yinan Li, Youming Qiao, Avi Wigderson, Yuval Wigderson, and Chuanqi Zhang. Connections between graphs and matrix spaces, 2022. arXiv:2206.04815.

[LWG+10] B. P. Lanyon, J. D. Whitfield, G. G. Gillett, M. E. Goggin, M. P. Almeida, I. Kassal, J. D. Biamonte, M. Mohseni, B. J. Powell, M. Barbieri, A. Aspuru-Guzik, and A. G. White. Towards quantum chemistry on a quantum computer. *Nature Chemistry*, 2(2):106–111, Jan 2010, 10.1038/nchem.483.

[MVM+23] A. Morvan, B. Villalonga, X. Mi, S. Mandrà, A. Bengtsson, P. V. Klimov, Z. Chen, S. Hong, C. Erickson, I. K. Drozdov, et al. Phase transition in random circuit sampling, 2023. arXiv:2304.11119.

[PDF+21] J. M. Pino, J. M. Dreiling, C. Figgatt, J. P. Gaebler, S. A. Moses, M. S. Allman, C. H. Baldwin, M. Foss-Feig, D. Hayes, K. Mayer, C. Ryan-Anderson, and B. Neyenhuis. Demonstration of the trapped-ion quantum CCD computer architecture. *Nature*, 592(7853):209–213, Apr 2021, 10.1038/s41586-021-03318-4.

[PMS+14] Alberto Peruzzo, Jarrod McClean, Peter Shadbolt, Man-Hong Yung, Xiao-Qi Zhou, Peter J Love, Alán Aspuru-Guzik, and Jeremy L O'brien. A variational eigenvalue solver on a photonic quantum processor. *Nature communications*, 5(1):4213, 2014, 10.1038/ncomms5213.

[PWD16] Alexandru Paler, Robert Wille, and Simon J. Devitt. Wire recycling for quantum circuit optimization. *Physical Review A*, 94(4):042337, Oct 2016, 10.1103/PhysRevA.94.042337.

[QC20] Google AI Quantum and Collaborators. Hartree-Fock on a superconducting qubit quantum computer. *Science*, 369(6507):1084–1089, Aug 2020, 10.1126/science.abb9811.

[RB01] Robert Raussendorf and Hans J Briegel. A one-way quantum computer. *Physical Review Letters*, 86(22):5188, 2001, 10.1103/PhysRevLett.86.5188.

[RN09] Stuart Russell and Peter Norvig. *Artificial Intelligence: A Modern Approach*. Prentice Hall, 2009.

[Sho94] Peter W. Shor. Algorithms for quantum computation: discrete logarithms and factoring. In *Proceedings 35th Annual Symposium on Foundations of Computer Science*, pages 124–134. IEEE, 1994. 10.1109/SFCS.1994.365700.

[Sim97] Daniel R. Simon. On the power of quantum computation. *SIAM Journal on Computing*, 26(5):1474–1483, Oct 1997, 10.1137/S0097539796298637.

[SJAG19] Sukin Sim, Peter D. Johnson, and Alán Aspuru-Guzik. Expressibility and entangling capability of parameterized quantum circuits for hybrid quantum-classical algorithms. *Advanced Quantum Technologies*, 2(12):1900070, Oct 2019, 10.1002/qute.201900070.

[WBC+21] Yulin Wu, Wan-Su Bao, Sirui Cao, Fusheng Chen, Ming-Cheng Chen, Xiawei Chen, Tung-Hsun Chung, Hui Deng, Yajie Du, Daojin Fan, et al. Strong quantum computational advantage using a superconducting quantum processor. *Physical Review Letters*, 127(18):180501, Oct 2021, 10.1103/PhysRevLett.127.180501.

[XLP+22] Mingkuan Xu, Zikun Li, Oded Padon, Sina Lin, Jessica Pointing, Auguste Hirth, Henry Ma, Jens Palsberg, Alex Aiken, Umut A. Acar, and Zhihao Jia. Quartz: Superoptimization of quantum circuits. In *Proceedings of the 43rd ACM SIGPLAN International Conference on Programming Language Design and Implementation*, page 625–640. Association for Computing Machinery, Jun 2022. 10.1145/3519939.3523433.

[XMP+23] Amanda Xu, Abtin Molavi, Lauren Pick, Swamit Tannu, and Aws Albarghouthi. Synthesizing quantum-circuit optimizers. *Proceedings of the ACM on Programming Languages*, 7(PLDI):835–859, Jun 2023, 10.1145/3591254.

[ZCC+22] Qingling Zhu, Sirui Cao, Fusheng Chen, Ming-Cheng Chen, Xiawei Chen, Tung-Hsun Chung, Hui Deng, Yajie Du, Daojin Fan, Ming Gong, et al. Quantum computational advantage via 60-qubit 24-cycle random circuit sampling. *Science Bulletin*, 67(3):240–245, Feb 2022, 10.1016/j.scib.2021.10.017.

[ZPW18] Alwin Zulehner, Alexandru Paler, and Robert Wille. An efficient methodology for mapping quantum circuits to the IBM QX architectures. *IEEE Transactions on Computer Aided Design of Integrated Circuits and Systems (TCAD)*, 38(7):1226–1236, Jun 2018, 10.1109/TCAD.2018.2846658.

A Compiling dynamic quantum circuit

In the same spirit of the main text, we can also consider starting from a dynamic quantum circuit and compiling it to a circuit with smaller width. However, this can be much more difficult and shall be related to the optimality of quantum circuit compilation, that is, determining whether a given dynamic quantum circuit can be further reduced. Therefore, it is worth noting that the applicability of our reducibility checking algorithm in Proposition 4, 6 and 9 is confined to static circuits. To illustrate this limitation, consider a dynamic circuit shown in Figure 30a. As evident from Figure 30b, within the DAG representation of this dynamic circuit, any terminal is reachable from any root. Consequently, it shall be concluded that this dynamic circuit is irreducible.

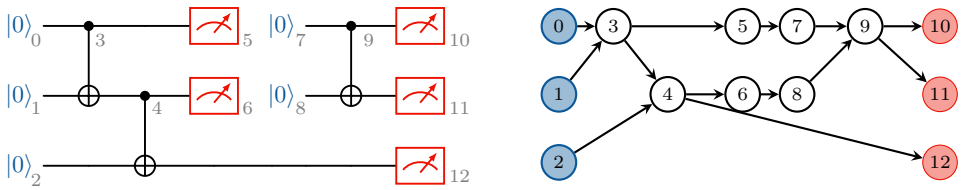

(a) An 'irreducible' dynamic circuit.

(b) DAG representation of the dynamic circuit

Figure 30: A dynamic quantum circuit and its DAG representation.

Nevertheless, further exploration reveals that the dynamic circuit can actually be compiled into the dynamic circuit shown in Figure 31, with the number of qubits reduced by one.

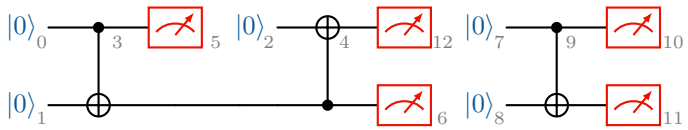

Figure 31: The dynamic quantum circuit reduced from the dynamic circuit in Figure 30a.

Interestingly, the dynamic circuit depicted in Figure 31 can be regarded as a dynamic circuit compilation outcomes of the static circuit in Figure 32a. As shown in Figure 32b, these two compilation schemes can be implemented by adding dashed orange edges and dashed green edges to the DAG representation of the static circuit in Figure 32a, respectively. Therefore, in the context of the compilation of a dynamic circuit, it is reasonable to commence with the conversion of the dynamic circuit into an equivalent static circuit. Following this conversion, the methodology in the main text can be employed to explore the existence of an enhanced compilation scheme in comparison to the original dynamic circuit.

The complete algorithm for converting a dynamic circuit to a static one is provided in Algorithm 9. The central concept involves assigning a new quantum register for each reset operation in the dynamic circuit. To elaborate, we traverse the dynamic circuit's instructions, and whenever we encounter a reset operation, we allocate a new qubit based on the current circuit width. All operations performed on the reset qubit after this reset operation are subsequently transferred to the newly allocated qubit. Through this process, the dynamic circuit can be transformed into an equivalent static circuit, essentially representing the reverse of our dynamic circuit compilation procedure. It is worth noting that Algorithm 9 can be adapted to accommodate dynamic circuits that feature classically controlled quantum gates with slight modification.

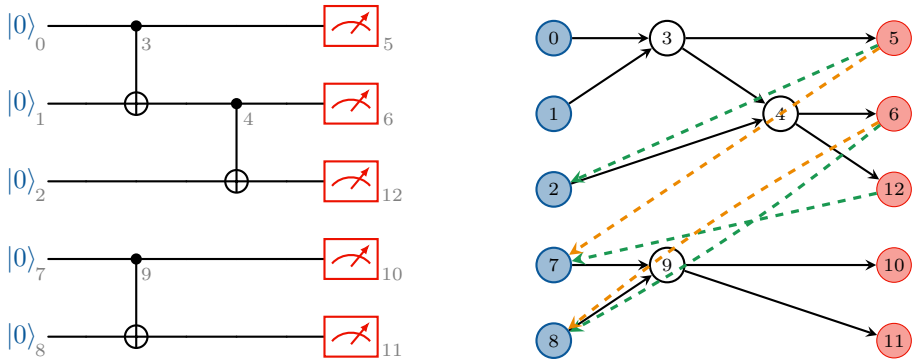

(a) The original reducible static circuit.

(b) Different compilation schemes.

Figure 32: A static quantum circuit that can be reduced to both the dynamic circuit in Figure 30a and Figure 31. The compilation scheme indicated by the dashed orange edges results in the dynamic circuit shown in Figure 30a, while the compilation scheme indicated by the dashed green edges leads to the dynamic circuit in Figure 31.

Algorithm 9: Converting dynamic circuit to static circuit

Input:

DynamicCircuit — the instruction list of a dynamic quantum circuit

Output:

StaticCircuit — the instruction list of the compiled quantum circuit

```
Let n be the dynamic quantum circuit width;
Initialize two empty lists StaticCircuit and Measurements;
foreach instruction in DynamicCircuit do
    if instruction is a measurement then
        Append instruction to Measurement;
    else if instruction is a reset then
        Record the value in QUBIT of instruction as ResetQubit;
        Initialize an empty list PostResets;
        Record all instructions subsequent to instruction in DynamicCircuit to PostResets;
        Remove all instructions subsequent to instruction from DynamicCircuit;
        foreach PostInstruction in PostResets do
            foreach Qubit in QUBIT of PostInstruction do
                if Qubit is equal to ResetQubit then Update Qubit to n;
            end
        end
        Update n to (n + 1);
        Append PostReset to DynamicCircuit;
    else if instruction is other single-/double-qubit gate then
        Append instruction to StaticCircuit;
    end
end
Append Measurement to StaticCircuit;
return StaticCircuit
```

B Implementation of DCKF algorithm

Since the DCKF algorithm described in [DCKFF22] is not publicly available, we implemented this algorithm based on our interpretation of their results. We observed that the causal cone of an output qubit q_i in their algorithm corresponds exactly to the set of roots that can reach the terminal of q_i. We effectively obtained this information by identifying all non-zero indices in the

i-th column of the biadjacency matrix of the quantum circuit.

Our initial step involved executing Algorithm 5 to obtain the biadjacency matrix and compute causal cones for all outputs. Subsequently, we applied their greedy strategy to determine the measurement order and identify how qubits are reused. It is important to note that, in order to complete a measurement, all qubits within its causal cone that have not yet been measured should be activated, while registers of all previously measured qubits are available for reuse.

Therefore, when a qubit q_i needed to be activated, we first identified all unoccupied registers from the existing ones. If an available register existed, q_i was loaded onto the first available one. Conversely, if all registers were occupied, a new register was initialized to accommodate q_i. Additionally, after the measurement of a qubit, the register it occupied was recycled for subsequent use. Upon the completion of all measurements in the input static circuit, the sequence in which registers were occupied was translated into a list of edges, which were subsequently incorporated into the DAG representation of the circuit.

Finally, the compilation process was completed by applying Algorithm 2. The full implementation of the DCKF algorithm is provided in Algorithm 10.

Algorithm 10: DCKF Algorithm

Input:

StaticCircuit the instruction list of a static quantum circuit

Output:

DynamicCircuit the instruction list of the compiled dynamic quantum circuit

Let n be the width of the static quantum circuit;
Run Algorithm 1 to get the DAG representation *Digraph* of the circuit;
Let *Roots* and *Terminals* be the set of roots and terminals, respectively;
Run Algorithm 5 to get the biadjacency matrix B of the simplified DAG of the circuit;
Initialize empty lists *CausalCones*, *Register*, *Occupation* and *AddedEdges*;
Initialize a set *UnmeasuredQubits* as $\{0, 1, ..., n-1\}$;
Initialize an empty set C_q;
for $i = 0$ **to** $n - 1$ **do**
    Let C be the set of row indices of non-zero entries in the i-th column of B;
    Append C to *CausalCones*;
end
for $t = 0$ **to** $n - 1$ **do**
    Initialize *ConeSize* as $n + 1$;
    foreach *Qubit* **in** *UnmeasuredQubits* **do**
        Calculate $Union = C_q \cup CausalCones[Qubit]$;
        if *the length of Union* $<$ *ConeSize* **then**
            Set *ConeSize* to the length of *Union*;
            Set *NextMeasure* to *Qubit*;
        end
    end
    Calculate *ActiveQubits* as $CausalCones[NextMeasure] - MeasureOrder$;
    foreach *Qubit* **in** *ActiveQubits* **do**
        if *Qubit not* **in** *Register* **then**
            Record all indeices of None in *Register* in *Available*;
            if *Available is not empty* **then**
                Record *Available*[0] as *Address*;
                Record the last element in *Occupation*[*Address*] as t;
                Append an edge (Terminals[t], Roots[*Qubit*]) to *AddedEdges*;
                Append *Qubit* to *Occupation*[*Address*];
            else
                Set *Address* to the length of *Register*;
                Append a list [*Qubit*] to *Occupation*;
            end
            Set *Register*[*Address*] to *Qubit*;
        end
    end
    Identify the index of *NextMeasure* in *Register* as m and set *Register*[m] to None;
    Append *NextMeasure* to *MeasureOrder*;
    Remove *NextMeasure* from *UnmeasuredQubits*;
    Calculate $C_q = C_q \cup CausalCones[NextMeasure]$;
end
Add *AddedEdges* to *Digraph* and get the *ModifiedGraph*;
Run Algorithm 2 to get the compiled circuit *DynamicCircuit*;
return *DynamicCircuit*